Food and Agriculture Organization of the United Nations

International Plant Protection Convention

ISPM 27
ANNEX 32

ENG

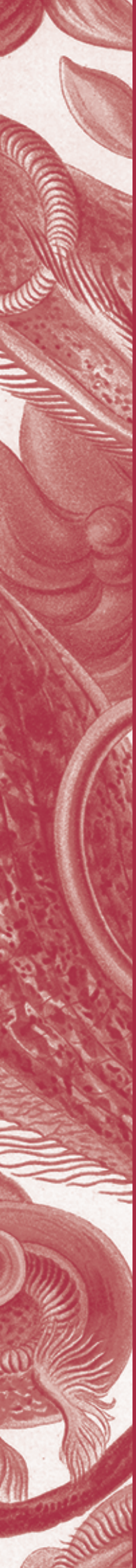

INTERNATIONAL STANDARD FOR PHYTOSANITARY MEASURES 27

DIAGNOSTIC PROTOCOL

DP 32: Genus *Ceratitis*

Produced by the Secretariat of the
International Plant Protection Convention (IPPC)

This page is intentionally left blank

This diagnostic protocol was adopted by the Standards Committee on behalf of the Commission on Phytosanitary Measures in August 2023.
The annex is a prescriptive part of ISPM 27.

ISPM 27
Diagnostic protocols for regulated pests

DP 32: Genus *Ceratitis*

Adopted 2023; published 2023

CONTENTS

1. Pest information 2
2. Taxonomic information 2
3. Detection 3
   3.1 Trapping 3
   3.2 Inspecting fruits 4
   3.3 Rearing larvae to obtain adults 4
4. Identification 4
   4.1 Morphological identification of adults 5
   4.1.1 Preparation of adults for identification 6
   4.1.2 Characters to identify adults to the genus *Ceratitis* 6
   4.1.3 Morphological identification of adults to pest species or complex 7
   4.2 Morphological identification of third-instar larvae 11
   4.2.1 Preparation of third-instar larvae for identification 11
   4.2.2 Characters to identify third-instar larvae of genus *Ceratitis* 13
   4.2.3 Characters to identify third instars of *Ceratitis capitata* 14
   4.2.4 Characters to identify third instars of *Ceratitis cosyra* 14
   4.2.5 Characters to identify third instars of the FARQ complex 15
   4.3 Molecular identification of *Ceratitis* species 17
   4.3.1 Sample preservation, preparation and DNA extraction for molecular tests 18
   4.3.2 Controls for molecular tests 18
   4.3.3 PCR amplification for DNA barcoding flies in the genus *Ceratitis* 19
   4.3.4 DNA sequence editing and quality control for DNA barcoding data 20
   4.3.5 Molecular tests for *Ceratitis capitata* 20
   4.3.6 Molecular tests for *Ceratitis cosyra* 25
   4.3.7 Molecular tests for the FARQ complex 26
5. Records 27
6. Contact points for further information 27
7. Acknowledgements 27
8. References 27
9. Figures 33

1. Pest information

The family Tephritidae is an economically important group of flies, commonly referred to as "fruit flies". The development of tephritid flies is dependent on the suitability of climatic conditions and the availability of host plants that can serve as mating locations, oviposition sites for eggs, and nutrient resources for developing larvae. The genus *Ceratitis* MacLeay consists of approximately 100 described species that are predominantly Afrotropical in distribution (De Meyer *et al.*, 2016). The genus consists of six subgenera (section 2).

The genus *Ceratitis* includes species that damage crops used for commercial and subsistence agriculture. The mated females oviposit eggs into fruit using a structure called an ovipositor. After the eggs hatch, larvae cause direct damage to the fruit by feeding on it. Indirect damage is caused by the increased susceptibility of the plant to opportunistic fruit pathogens resulting from injuries during oviposition into the fruit and from larval feeding damage. *Ceratitis* species can be generalist feeders (polyphagous), specialists that feed on a particular species (monophagous), or specialists that feed on a lineage of plant species (i.e. stenophagous and oligophagous). However, the known relationship between many species of *Ceratitis* and their host plants is incomplete. Some host-use records are from field observations that still require confirmation on infested fruits (see ISPM 37 (*Determination of host status of fruit to fruit flies (Tephritidae)*) and some *Ceratitis* species may infest a wider range of hosts than currently reported.

Six economically important *Ceratitis* species are included in this diagnostic protocol based on their distribution and status as polyphagous pests (White and Elson-Harris, 1992; De Meyer *et al.*, 2016). The most destructive global species in the genus is the generalist *C.* (*Ceratitis*) *capitata* (Wiedemann). Native to sub-Saharan Africa (De Meyer *et al*., 2002), *C. capitata* has successfully invaded other regions of Africa, Hawaii, South America, Central America, Australia and countries of the Mediterranean region. Hundreds of plant species have been reported as hosts for *C. capitata* (White and Elson-Harris 1992; Liquido, McQuate and Suiter, 2016; USDA, 2023).

The protocol also includes *C.* (*Ceratalaspis*) *cosyra* (Walker), which is a pest of many fruit hosts such as *Annona muricata* (soursop), *Eriobotrya japonica* (loquat), *Mangifera indica* (mango), *Prunus persica* (peach) and *Psidium guajava* (guava). It is found throughout much of sub-Saharan Africa and is reported to be a cryptic species complex (Virgilio *et al.*, 2017).

The other four species included in the protocol are *C.* (*Pterandrus*) *fasciventris* (Bezzi), *C.* (*Pterandrus*) *anonae* Graham, *C.* (*Pterandrus*) *rosa* Karsch and *C.* (*Pterandrus*) *quilicii* De Meyer *et al*. These infest a wide range and a large number of commercially grown hosts. The distribution for each of these four species includes multiple countries across sub-Saharan Africa; although each species has a different distribution range, these ranges can overlap (De Meyer *et al.*, 2015; De Meyer *et al.*, 2016). These four species are included in a taxonomic species complex called the "FARQ complex" because of their high morphological and molecular similarity (Barr and McPheron, 2006; Virgilio *et al.*, 2008; Zhang *et al.*, 2021).

2. Taxonomic information

Name: *Ceratitis* MacLeay, 1829

Synonyms: none

Taxonomic position: Insecta, Diptera, Tephritidae, Dacinae, Ceratitidini

The genus consists of six subgenera as proposed by Hancock (1984) and revised in several studies (De Meyer, 1996, 1998, 2000; De Meyer and Copeland, 2001; De Meyer and Freidberg, 2005):

Ceratitis (*Acropteromma*) (Bezzi, 1926)
Ceratitis (*Ceratalaspis*) Hancock, 1984
Ceratitis (*Ceratitis*) MacLeay, 1829
Ceratitis (*Hoplolophomyia*) Bezzi, 1926

Ceratitis (*Pardalaspis*) Bezzi, 1918
Ceratitis (*Pterandrus*) Bezzi, 1918

Acropteromma and *Hoplolophomyia* are monotypic subgenera (De Meyer, 1999, 2005; De Meyer and Copeland, 2001). *Ceratalaspis* and *Pterandrus* are not monophyletic subgenera (De Meyer, 2005; Barr and McPheron, 2006; Barr and Wiegmann, 2009). *Pterandrus* is divided into two sections (A and B) and is paraphyletic with respect to subgenus *Ceratitis* (Barr and Wiegmann, 2009). *Pterandrus* section B and subgenus *Ceratitis* form a monophyletic clade. The subgenus *Pardalaspis* is monophyletic.

Common names and synonyms of the *Ceratitis* species included in this protocol are in Table 1.

Table 1. Common names and synonyms (and other names) of species of major economic importance belonging to the genus *Ceratitis* and included in this diagnostic protocol

Species	Common name	Synonyms (and other names)
Ceratitis (*Pterandrus*) *anonae* Graham, 1908	-	*Ceratitis pennipes* Bezzi, 1908 *Pterandrus anonae* (Graham, 1908)
Ceratitis (*Ceratitis*) *capitata* (Wiedemann, 1824)	Mediterranean fruit fly, medfly	*Tephritis capitata* Wiedemann, 1824 *Ceratitis citriperda* MacLeay, 1829 *Pardalaspis asparagi* Bezzi, 1924
Ceratitis (*Ceratalaspis*) *cosyra* (Walker, 1849)	mango fruit fly	*Trypeta cosyra* Walker, 1849 *Ceratitis giffardi* Bezzi, 1912 *Pardalaspis giffardi* var. *sarcocephali* Bezzi, 1924 *Pardalaspis parinarii* Hering, 1935
Ceratitis (*Pterandrus*) *fasciventris* (Bezzi, 1920)	-	*Pterandrus rosa* var. *fasciventris* Bezzi, 1920 *Pterandrus flavotibialis* Hering, 1935
Ceratitis (*Pterandrus*) *quilicii* De Meyer *et al.*, 2016	Cape fruit fly	(*Ceratitis rosa* R2, 'highland')*
Ceratitis (*Pterandrus*) *rosa* Karsch, 1887	Natal fruit fly	*Pterandrus rosa* (Karsch, 1887) (*Ceratitis rosa* R1, 'lowland')*

*Note: ** Prior to De Meyer *et al.* (2016), *C. quilicii* and *C. rosa* were considered to be conspecific.

3. Detection

Fruit flies of the genus *Ceratitis* are detected mainly by trapping adults or by finding eggs and larvae in fruits. Male attractant lures are commonly used for *C. capitata* adults (Tan *et al.*, 2014) and may be useful for pest species in the subgenera *Ceratitis* and *Pterandrus* but are not effective for all species in the genus (De Meyer, 1999). The most commonly used lures are trimedlure (for *Ceratitis capitata* and members of the *Ceratitis* FARQ complex), terpinyl acetate (for *C. cosyra*) and enriched ginger oil lure (Mwatawala *et al.*, 2013; Manrakhan *et al.*, 2017). Other male attractants have been evaluated, such as methyl eugenol for species in the subgenus *Paradalaspis* (De Meyer, 1999). In addition, food-based attractants have been reported to be effective for many adult flies (Epsky, Kendra and Schnell, 2014; Manrakhan, 2017).

Immature stages (eggs and first-, second- and third-instar larvae) can be found during inspection of fruits. After completing development, larvae exit the fruit, and the immobile pupal stage develops elsewhere (e.g. in leaf litter, soil, or the packaging of containers).

3.1 Trapping

Guidance on trapping *Ceratitis* fruit flies, including use of attractants for trapping, such as synthetic food attractants and hydrolysed protein substances, is given in Appendix 1 of ISPM 26 (*Establishment of pest free areas for fruit flies (Tephritidae)*).

3.2 Inspecting fruits

Signs of fruit fly infestation are the presence of soft areas, dark stains, dark pin spots, rot, holes or injuries that might be caused by oviposition or larval feeding activities. To detect punctures made by female flies during oviposition, fruits can be examined under a stereomicroscope by an expert. If larval exit holes are observed, puparia may be detected in the packaging of the fruit. Third instars may not be present when unripe fruit is collected and packed; however, this fruit might host eggs and first or second instars, which are more difficult to detect. On potentially infested fruit showing typical punctures made by ovipositing female flies, eggs and larvae may be seen when cutting the fruit open.

Once detected, larvae may be reared to adults for identification (section 3.3). Rearing of adults is required to accurately identify a fly to species level with morphological techniques. Even if there are no signs of fruit fly infestation, an incubation can be conducted as an oviposition mark is often difficult to recognize.

3.3 Rearing larvae to obtain adults

Larvae can be reared to adults by placing infested fruits in cages containing a pupation medium (e.g. damp vermiculite, sand or sawdust) on the bottom. Incubation temperatures around 24 °C have been used to rear *C. capitata* from fruit in Africa (Copeland *et al.*, 2002) and relative humidities above 75% have been used to rear adults of three *Ceratitis* species (Duyck, David and Quilici, 2006). The cages can be covered with cloth or fine mesh. Once the larvae emerge from the fruit, they will move to the pupation medium. Each sample should be observed, and pupae collected daily. The collected pupae can be placed in containers with the pupation medium, and the containers covered with a tight lid that enables proper ventilation. Once the adults emerge, they must be kept alive for several days to ensure that the integument and wings acquire the rigidity and characteristic coloration of the species. Flies can be fed with honey and water or a mix of sugar, yeast, wheat germ and water. The adults are then killed by freezing, or by exposure to ethyl acetate or other killing agents appropriate for morphological examination, and then mounted on pins. If molecular analysis is to be performed, there are additional methods for specimen handling (section 4.3.1).

Before mounting (before specimens harden), it is useful to gently squeeze the apical part of the preabdomen with forceps, then squeeze the base of the oviscape to expose the aculeus tip for females. Alternatively, this will need to be dissected later in flies. The aedeagus is not commonly used for identification of *Ceratitis* males.

4. Identification

Identification at the level of species or species complex requires morphological examination of adult flies or molecular analysis. For some species, accurate identification can only be completed for male specimens because the female form has not been described or females lack diagnostic features. In addition to keys developed for species in each subgenus (De Meyer, 1996, 1998, 2000; De Meyer and Freidberg, 2005), an online multi-entry Lucid key to frugivorous flies of Africa is available that can be used to identify *Ceratitis* species (Virgilio, White and De Meyer, 2014).

It is not reliable to morphologically identify eggs, most larvae or pupae to species level. There are descriptions of third instars for some species but not all species of economic importance in the family. This lack of descriptions could impact identification to genus level (Steck and Ekesi, 2015). These descriptions of the third instar can be used to discriminate among the described pest species (White and Elson-Harris, 1992; Steck and Ekesi, 2015) but not to distinguish with reliability one pest species from all other pest species. This is true of all *Ceratitis* species. The descriptions of third-instar *Ceratitis* are usually based on laboratory colony material and might not accurately represent the true diversity of the species (Steck and Ekesi, 2015). The most reliable methods for identifying species are rearing larvae to the adult stage or molecular analysis.

A key to identifying economically important genera based on third instars has been published (White and Elson-Harris, 1992), and an online identification tool that includes 81 economically important

species of 13 genera is available (Carroll *et al*., 2004). *Ceratitis* is the only economically important genus from the tribe Ceratitidini included in the key and the diversity of each genus in the key is based on examination of a limited number of species with larval descriptions available. Steck and Ekesi (2015) reported that a character previously used to distinguish *Ceratitis* and *Bactrocera* larvae was based on limited taxon sampling. Morphological examination of a third instar can provide diagnostic information but for first records of a species additional molecular diagnostic information will be needed.

Host and geographical distribution records are not included in the current protocol as diagnostic features of *Ceratitis* species because the values are incomplete for many species and subject to change over time. The scope of the protocol is therefore limited to morphological (section 4.1 and section 4.2) and molecular (section 4.3) characters.

Molecular methods for *Ceratitis* species identification have been published for several of the most destructive, polyphagous pests: *C. capitata* (Barr *et al.*, 2006; Huang *et al.*, 2009; Barr *et al*., 2012; Dhami *et al.*, 2016), *C. cosyra* (Barr *et al.*, 2006; Virgilio *et al.*, 2017), and the FARQ complex – *C. fasciventris*, *C. anonae*, *C. rosa* and *C. quilicii* (Virgilio *et al.*, 2019; Zhang *et al*., 2021). These studies have considered the molecular phylogeny of the genus (Barr and McPheron, 2006; Barr and Wiegmann, 2009; Erbout *et al.*, 2011) to include species that would have a greater probability of a false positive with a target pest or lead to incorrect interpretation of a diagnostic result. Only methods that have included sufficient taxonomic sampling to demonstrate analytical specificity are included in this diagnostic protocol. These include a real-time polymerase chain reaction (PCR) method for *C. capitata* (Dhami *et al.*, 2016) and DNA barcoding methods for the identification of *C. capitata*, *C. cosyra* and the FARQ complex using DNA sequencing of part of the mitochondrial cytochrome c oxidase I (*COI*) gene (section 4.3).

DNA barcode records for other *Ceratitis* species are reported in the literature (Barr *et al.*, 2012; Virgilio *et al.*, 2012) and can be accessed using DNA databases. Formal examination of reference data specificity has not been reported for the species not included in this protocol. Methods to identify insects to the level of genus *Ceratitis* based on DNA barcodes have not been formally described or published; consequently, methods to identify the genus are not included in this protocol.

Population genetic analysis of *C. capitata* has revealed several methods for evaluating geographical association (Gasparich *et al.*, 1997; Davies, Villablanca and Roderick, 1999; Bonizzoni *et al.*, 2000, 2004; Meixner *et al.*, 2002; Barr, 2009; Ruiz-Arce *et al.*, 2020) or determining the laboratory colony source of a fly (San Andrés *et al.*, 2007; Juan-Blasco *et al.*, 2013; Sim *et al.*, 2017; Catalá-Oltra *et al.*, 2020). The accuracy of methods can depend on changing frequencies of genotypes over time and changes in the production or source of laboratory colonies used for the sterile insect technique. These are not, therefore, included in the current protocol.

The destruction of insect tissue for DNA-based identification can preclude morphological examination unless care is taken to retain the remaining body parts needed for such examination. The use of a fly leg for DNA extraction is recommended for some species when molecular data are to be collected, but the remaining body parts of the specimen should be saved for morphological analysis. The presence of characters on fore and mid legs are diagnostically informative in the genus, and at least one leg of each pair should be retained for morphological examination. When a larva is needed for morphological examination, excision of tissue from the midsection should be performed to collect molecular data. For guidance on preparing a specimen for molecular study, see section 4.3.1.

Molecular methods can be used for all life stages. Morphological identification methods are not available for eggs and pupae.

4.1 Morphological identification of adults

The diagnostic characters required to complete identification to the species covered by this protocol and to the genus are provided below. Additional resources on general characters for tephritid fruit fly identification are provided in White and Elson-Harris (1992). The terminology for morphological characters followed is according to the glossary of White *et al*. (1999).

4.1.1 Preparation of adults for identification

Proper preparation of specimens is essential for accurate morphological identification. General instructions on the preparation of adult fruit fly specimens are given by White and Elson-Harris (1992).

Every attempt should be made to preserve all characters on at least one side of the centre line, regardless of the mounting method (Foote, Blanc and Norrbom, 1993).

Characters on the head, wing, leg, thorax and abdomen of a fly can be examined from pinned specimens under magnification using a stereomicroscope at ≥20×. This magnification level is appropriate for observing spot and colour patterns and wing morphology (section 4.1.2).

Wing characters can usually be observed without slide mounting, so mounting is not recommended as a general practice. It may be necessary for morphometric studies, but it is not necessary to observe the characters used in section 4.1.3. If permanent slide mounts are made, it is recommended that one of the wings be cut off from its base (the right wing is preferred because it facilitates comparison with images reported in the literature and this diagnostic protocol).

Structures of the ovipositor, such as aculeus shape and length, have not been used consistently as important taxonomic characters at the genus or species level of many *Ceratitis*, except for the aculeus tip which has been used for some groups in the subgenus *C.* (*Ceratalaspis*). These structures are not included in this protocol for diagnosis.

4.1.2 Characters to identify adults to the genus *Ceratitis*

There is no unambiguous character that differentiates all representatives of the genus *Ceratitis* from any of the other closely related genera within the Dacinae. The combination of the presence of acrostichal setae (sometimes referred to as prescutellar setae) (Figure 1), presence of basal scutellar setae (Figure 2) and the short appendix of the wing cell bcu (the posterior cubital cell, sometimes referred to as the cell cup) with a constriction at the base (Figure 3) excludes other dacine genera that contain pest species (such as *Bactrocera* Macquart, *Dacus* Fabricius and *Zeugodacus* Hendel) as well as any other non-dacine genera.

The following combination of characters differentiates representatives of the genus *Ceratitis* from other dacine genera with a similar appearance:

- The scutellum of most *Ceratitis* species is rounded and swollen (viewed from the side) (Figure 2). *Carpophthoromyia* Austen and *Perilampsis* Bezzi have a flattened and less rounded scutellum (see Figure 4).
- The scutellum of *Ceratitis* species has three dark apical markings, which can be clearly separated (Figure 2) or partially fused (Figure 5). In some cases, they cover most of the apical and central part of the scutellum (Figure 6), while in some other cases they are reduced to small dark spots (Figure 7). This character excludes species of the genus *Capparimyia* Bezzi, which have only two dark apical markings (Figure 8), and several species of the genus *Trirhithrum* Bezzi that have a completely black scutellum (Figure 9). It also excludes some species of the genus *Neoceratitis* Hendel that have a single dark apical marking (Figure 10).
- The majority of *Ceratitis* species have a typical wing banding pattern consisting of an anterior apical band, a discal band and a subapical band (Figure 3). In some cases, an additional posterior apical band is present (Figure 11). A few *Ceratitis* species have wing banding that deviates from the normal pattern (i.e. *C. divaricata* (Munro, 1933), *C. flexuosa* (Walker, 1853), *C. munroanum* (Bezzi, 1926), *C. taitaensis* De Meyer and Copeland, 2016, *C. whartoni* De Meyer and Copeland, 2009) but none of them is of economic significance. The typical wing banding is also shared by some *Trirhithrum* and *Neoceratitis* species. The latter two genera can be separated from *Ceratitis* by the banding being dark black to black-brown, combined with the presence of a posterior apical band (Figure 12) or at least a "tooth-shaped" triangular extension on the anterior apical band (Figure 13). *Ceratitis* species usually have yellow to brown wing bands (Figure 3 and Figure 11).

Phylogenetic studies have indicated that at least some *Trirhithrum* species cluster within the *Ceratitis* genus (see Virgilio *et al.*, 2015). Thus, the generic concept of both *Ceratitis* and *Trirhithrum*, and the species to be included in each of these higher taxa, needs revision.

4.1.3 Morphological identification of adults to pest species or complex

For the purposes of this protocol, a number of characters useful for the identification of adult flies have been retrieved from the different revisions of subgenera (De Meyer 1996, 1998, 2000; De Meyer and Freidberg, 2005) and from the subsequent inclusion in the identification tool developed by Virgilio, White and De Meyer (2014). The diagnostic character states for the six economically important *Ceratitis* species included in this protocol are listed in Table 2, with reference to relevant images illustrating the states.

Table 2. Diagnostic morphological characters of adults of *Ceratitis* species in this protocol

Character	**Species**					
	C. anonae	***C. capitata***	***C. cosyra***	***C. fasciventris***	***C. quilicii***	***C. rosa***
Both sexes, postpronotal lobe	Unicolorous (Figure 14 & Figure 15)	Pale with black median spot (Figure 16 & Figure 17)	Pale with black median spot (Figure 16 & Figure 17)	Unicolorous (Figure 14 & Figure 15)	Unicolorous (Figure 14 & Figure 15)	Unicolorous (Figure 14 & Figure 15)
Both sexes, scutellum, apical spots	Three separate spots (Figure 18)	One merged spot (Figure 19)	Three separate spots (Figure 18)	Three separate spots (Figure 18)	Three separate spots (Figure 18)	Three separate spots (Figure 18)
Both sexes, scutum	Greyish to greyish-brown ground colour, with indistinct darker markings (Figure 20)	Grey ground colour with distinct black markings (Figure 21)	Yellow-orange to orange ground colour with distinct black markings (Figure 22) (black markings can sometimes be strongly reduced)	Greyish to greyish-brown ground colour, with indistinct darker markings (Figure 20)	Greyish to greyish-brown ground colour, with indistinct darker markings (Figure 20)	Greyish to greyish-brown ground colour, with indistinct darker markings (Figure 20)
Both sexes, wing, anterior apical band	Completely separated from discal band (Figure 23 & Figure 24)	Completely separated from discal band (Figure 23 & Figure 24)	Connected with discal band (Figure 25), at most partially separated (Figure 26)	Completely separated from discal band (Figure 23 & Figure 24)	Completely separated from discal band (Figure 23 & Figure 24)	Completely separated from discal band (Figure 23 & Figure 24)

(Table 2 continued on next page)

(Table 2 continued)

Character	Species					
	C. anonae	***C. capitata***	***C. cosyra***	***C. fasciventris***	***C. quilicii***	***C. rosa***
Both sexes, abdomen, tergum 3	With black-brown band (Figure 27)	Without black-brown band (Figure 28)	Without black-brown band (Figure 28)	With black-brown band (Figure 27)	With black-brown band (Figure 27)	With black-brown band (Figure 27)
Male, head, lower orbital seta	Bristle-like, not modified apically (Figure 29 & Figure 30)	Modified, flattened at apex (Figure 31 & Figure 32)	Bristle-like, not modified apically (Figure 29 & Figure 30)	Bristle-like, not modified apically (Figure 29 & Figure 30)	Bristle-like, not modified apically (Figure 29 & Figure 30)	Bristle-like, not modified apically (Figure 29 & Figure 30)
Male, leg, fore femur	Posteriorly with dispersed setae (Figure 33 & Figure 34)	Posteriorly with brush of dense setae (Figure 35)	Posteriorly with dispersed setae (Figure 33 & Figure 34)	Posteriorly with dispersed setae (Figure 33 & Figure 34)	Posteriorly with dispersed setae (Figure 33 & Figure 34)	Posteriorly with dispersed setae (Figure 33 & Figure 34)
Male, leg, mid femur	Ventrally with row of long stout setae (“feathering”) (Figure 36)	Ventrally with few dispersed long but thin setae (Figure 37)	Ventrally with few dispersed long but thin setae (Figure 37)	Ventrally with few dispersed long but thin setae (Figure 37)	Ventrally with few dispersed long but thin setae (Figure 37)	Ventrally with few dispersed long but thin setae (Figure 37)

(Table 2 continued on next page)

(Table 2 continued)

Character	Species					
	C. anonae	***C. capitata***	***C. cosyra***	***C. fasciventris***	***C. quilicii***	***C. rosa***
Male, leg, mid tibia	Dorsal and ventral sides with row of long black stout setae (feathering) for more than three-quarters of entire length (Figure 38)	Dorsal and ventral sides with few dispersed short setae (Figure 39)	Dorsal and ventral sides with few dispersed short setae (Figure 39)	Dorsal and ventral sides with row of long stout setae (feathering) for less than half of apical part (Figure 40)	Dorsal and ventral sides with row of long stout setae (feathering) for more than half but less than three-quarters of entire length (Figure 41)	Dorsal and ventral sides with row of long stout setae (feathering) for more than half but less than three-quarters of entire length (Figure 42)
Male, leg, mid tibia	Pale to brownish over entire length (Figure 38)	Pale over entire length (Figure 39)	Pale over entire length (Figure 39)	Usually pale, at most area between feathering partially darker yellow to brownish (Figure 40)	Pale except area between feathering where darker coloured; dark colour not reaching dorsal part (red arrow in Figure 41)	Pale except area between feathering where darker coloured; dark colour reaching dorsal part (red arrow in Figure 42)
Female, anepisternum	With partly dark setulae (pilosity) in lower half (Figure 43)	Setulae (pilosity) entirely pale (Figure 44)	Setulae (pilosity) entirely pale (Figure 44)	Setulae (pilosity) entirely pale (Figure 44)	Setulae (pilosity) entirely pale (Figure 44)	Setulae (pilosity) entirely pale (Figure 44)
Female, leg, fore femur	Posteriorly with few dark hairs between posterior and posterodorsal rows of setae (Figure 33)	Posteriorly without dark hairs between posterior and posterodorsal setae (Figure 34)	Posteriorly without dark hairs between posterior and posterodorsal setae (Figure 34)	Posteriorly without dark hairs between posterior and posterodorsal setae (Figure 34)	Posteriorly without dark hairs between posterior and posterodorsal setae (Figure 34)	Posteriorly without dark hairs between posterior and posterodorsal setae (Figure 34)

4.2 Morphological identification of third-instar larvae

As explained at the beginning of section 4, identification of flies based on examination of the third-instar life stage is not sufficient to complete accurate species identification under all circumstances. Larval descriptions are not available for all species that could be confused for a pest, and descriptions are based on laboratory-reared colonies that might not represent the true variation of the species (Steck and Ekesi, 2015). However, a diagnosis to the genus or species that is based solely on larval morphology could be appropriate when screening for a pest where its presence is expected based on prior information and closely related species that could be mistaken for the pest are absent. Molecular analysis (section 4.3) should be performed to complete the identification of a larva when the diagnosis is intended to confirm a new record of pest presence. Molecular methods in this protocol will not be sufficient for cryptic species where rearing to adults is necessary, especially to confirm a first record.

Morphological characters of third instars are published for several *Ceratitis* species. These descriptions can be used to discriminate among species that have been studied. They can also be used to provide additional support to the identification if the identification is based on molecular methods. In this protocol, a description of third instars for the genus *Ceratitis* is provided that has been extrapolated from published species descriptions: this may be of value in supporting identifications.

When a larva is detected in fruit, identification of the instar stage is not always certain. The fully developed second instar and newly moulted third instar of a fly species can be the same length: the third-instar *Ceratitis*, for example, can be as small as 3.2 mm in length for some species, which can overlap with the length of the second instar in those species (Steck and Ekesi, 2015). Typical relative sizes of the egg and three instars are shown in Figure 45. The best characters to separate instars in all species are the absolute sizes of the cephaloskeleton and spiracles: they never overlap between instars (see Figure 46 on how size is measured). However, these data are not published for second or first instars of most species. Another differentiating feature between third and second instars of *Ceratitis* is the relative size of the mouthhook subapical tooth: in the third instar the subapical tooth is very small compared to the apical tooth (Figure 46), but in the second instar it is subequal (Figure 47).

Larvae can be examined using a stereomicroscope, compound optical microscope and scanning electron microscope (SEM). General examination for initial screening can be accomplished using the stereomicroscope, but slide-mounted specimens under a compound microscope or SEM are needed to complete genus and species identification. The most detailed images and illustrations reported in the literature are from SEM examination of specimens.

4.2.1 Preparation of third-instar larvae for identification

Larvae can be prepared for morphological examination by first killing them in very hot or boiling water and then storing them in 70% ethanol.

The live larvae can be killed by placing in water at $\geq$65 °C for at least two minutes, cooled to room temperature and then preserved in 70% ethanol. If larvae turn partially or completely black after one day, the hot water treatment was inadequate, and the water temperature or treatment time should be increased. The larval cuticle may split open on one side near the head, but this is inconsequential for identification purposes. Splitting is minimized if the larvae are run through a graduated alcohol series of 35%–50%–70% ethanol for two hours each, with an additional change to fresh 70% alcohol. It is advisable to include a label in the storage vial with all sampling information. These samples are ready for examination under a stereomicroscope or subsequent preparation for slide mounting or examining under an SEM.

Larvae that are to be used for morphological analysis alone can be saved in 70% ethanol after boiling. Those larvae that are to be used for both morphological and molecular analysis can have tissue excised (section 4.3.1) and saved in ≥95% ethanol in a freezer (≤-20 °C) until DNA is extracted and the remaining anterior and posterior sections saved in 70% ethanol.

4.2.1.1 Preparing unmounted larvae for optical microscope examination

Morphological examination of larvae can be performed on unmounted specimens using a stereomicroscope. After intact larvae are removed from alcohol and blotted dry, their external features – such as oral ridges, anterior and posterior spiracles, and anal lobes – can be examined. Counts of oral ridges and lobes of the anterior spiracle can be made, as well as observations of characters such as shapes of spiracles and anal lobes, orientation and length and width measurements of posterior spiracular slits, and presence or absence of dorsal spinules and caudal ridges. Fine details of the facial mask (preoral lobes, oral ridges and their edges, accessory plates) of an unmounted larva can be observed by using a transmitted-light compound microscope. A clean, dry larva is placed on a piece of facial tissue on a glass slide and the head is observed at 100× magnification. Specimens should be re-wetted with alcohol as needed to prevent shrivelling during examination.

4.2.1.2 Preparing larvae for slide mounting and examination using a compound microscope

Morphological examination can be performed on slide-mounted larvae using a compound microscope with objective 20×, 40× or higher. These slide-mounted larvae can be examined for external morphology (e.g. anterior and posterior spiracles, oral ridges) as well as internal structures such as the cephaloskeleton. However, slide mounting larvae can preclude subsequent higher resolution analysis of morphological characters observable using SEM. It is therefore not recommended to slide mount all specimens representing a sample or the only larva available for diagnosis; unmounted larvae should be kept for future analysis.

To prepare specimens for slide mounting, it is necessary to remove (clear) all the internal tissues to allow observation of the cuticle, oral opening, cephaloskeleton, anterior and posterior spiracles, and anal lobes. First, two incisions are made in the larva: one laterally through the thoracic segments, and one between the posterior spiracles and anus. Then the incised larva is immersed in hot 10% NaOH or 10% KOH solution for 10–15 min or until most internal tissues are visibly digested. After digestion, the remaining internal debris is carefully removed using forceps and the specimen flushed with distilled water under a stereomicroscope. The cephaloskeleton is extracted through the lateral incision on the thorax.

Cleared specimens can be placed in glycerine on a glass depression slide with a cover slip for examination or imaging and recording of measurement data under a compound microscope (Figure 48). Afterwards, specimens can be retained as vouchers by returning them to alcohol in a labelled vial, or permanent slide mounts can be made using Canada balsam or Euparal following standard methods. For permanent mounts, care must be taken to position and stabilize the specimen in the proper orientation before adding the cover slip, otherwise it may be impossible to get realistic images or accurate measurements after the specimen dries in place. Slides must be allowed to dry for several days or weeks (the time can be reduced by using an oven), but they can be examined under the microscope at low magnification immediately after mounting. Slides should be labelled.

4.2.1.3 Preparing larvae for SEM examination

For observation using an SEM, the specimens (stored in alcohol) should first be completely dehydrated by running through a series of ethanol rinses – 70%, 80%, 95%, and two or three changes of absolute ethanol – followed by one or two rinses in ethyl acetate and air-dried (or critical-point dried after the alcohol dehydration series), then coated with gold–palladium and mounted on a stub (Carroll and Wharton, 1989). If the larval specimen has not been cut or punctured before the ethanol rinses, then two to three lateral punctures should be made with a minuten pin to allow alcohol to permeate the tissues. The duration of each ethanol rinse for a larva with punctures should be at least two hours. If the midsection of the larval specimen has been excised and removed (section 4.3.1), then alcohol permeates the tissue more quickly and each rinse step should have a duration of 15 minutes. Similar techniques can be found elsewhere (e.g. Frías *et al.*, 2006; Frías, Selivon and Hernández-Ortiz, 2008; Frías Lasserre, Hernández Ortiz and López Muñoz, 2009).

4.2.2 Characters to identify third-instar larvae of genus *Ceratitis*

Diagnosis: dorsolateral pair of sensilla parallel to maxillary palpus; preoral lobes elongate and petal-like, preoral organ ringed with petal-like lobes; preoral teeth absent; mouthhook apical tooth ventrally grooved, conical subapical tooth present or absent, mouthhook basally elongate, dental sclerite present; oral ridges with scalloped edges, accessory plates, when present, in single series; anterior spiracle tubules in single sinuous row, in profile flat to convex centrally; rimae of posterior spiracles approximately 2.5–3.5 times longer than wide; caudal ridge present; thin, dark, sclerotized line absent on caudal segment ventral to spiracles; live, mature third instars display skipping (jumping) behaviour. Important exceptions are noted below under the individual species notes.

Fruit fly larval descriptive terminology has evolved over the years. Useful references include Teskey (1981), Steck and Wharton (1988), White and Elson-Harris (1992), White *et al.* (1999), Carroll *et al.* (2004), Rodriguez *et al.* (2021) and Steck *et al.* (2022). The figures in this protocol illustrate the usage employed here and the diagnostic and key features listed above and below.

A generalized fruit fly larval habitus (Figure 49) shows the anatomical disposition of the pseudocephalon, thoracic segments and abdominal segments, together with the locations of important key features such as the mouthhooks, spinules, anterior and posterior spiracles, and anal lobes.

The pseudocephalon (head) of a fruit fly larva has two prominent protuberances (cephalic lobes), each bearing an antennal sensory organ, a dorsolateral pair of sensilla, and a maxillary palpus. The pair of dorsolateral sensilla are arranged parallel to the maxillary palpus in *Ceratitis* and other Dacinae, which differs from the perpendicular arrangement seen in *Anastrepha* (Figure 50, Figure 51 and Figure 52). They can be observed using either an SEM or a compound microscope.

The preoral lobes are present just anterior to the mouth opening, and laterally adjacent to them are the preoral organ and associated lobes. In *Ceratitis* larvae, the preoral organ is a small cylindrical lobe bearing sensilla that is ringed by several petal-like lobes, referred to as the preoral lobes, that extend medially (Figure 53). The preoral organ and lobes are similar to those of *Bactrocera*, but differ from those of *Dacus* and *Zeugodacus* larvae (Figure 54), in which the preoral lobes are elongated with toothed margins identical to the oral ridges (Steck *et al*., 2022), and from those of *Anastrepha* larvae (Figure 55), in which the sensilla of the preoral organ are on the lateral ends of an elongate, undifferentiated preoral lobe (Rodriguez *et al*., 2021). These features can be observed in detail under an SEM and sometimes crudely under a dissecting or compound microscope.

Preoral teeth are absent in Dacinae. They occur in one tribe of the Trypetinae – the Carpomyini (*Rhagoletis*, *Carpomya*) – and consist of one to several stout sclerotized teeth on the posterior surface of the preoral organ. They can be observed using either an SEM or a light microscope (Figure 56 and Figure 57).

Most of the cephaloskeleton is internal and not visible until the specimen is cleared. Only part of the mouthhook is visible externally. In *Ceratitis* species, the mouthhook has a large apical tooth and a small subapical tooth. However, the subapical tooth may be imperceptibly small (visible only under an SEM) or entirely absent in some specimens of *C. capitata* and *C. rosa*. The subapical tooth is always absent in *Anastrepha* and most pest species of *Bactrocera* (exceptions with subapical tooth include *B.* (*Notodacus*) *xanthodes* and *B.* (*Javadacus*) *trilineata*) (Figure 58 and Figure 59). The ventral shape of the apical tooth can easily be seen under an SEM, but it is not apparent under a light microscope. It is ventrally grooved in *Ceratitis* but tusk-like in *Dacus* and some *Zeugodacus* spp. (Figure 58, Figure 59 and Figure 60). The posterior part of the mouthhook is extended into an elongate neck beyond the ventral protuberance in *Ceratitis* and other Dacinae but is truncate posteriorly in Trypetinae (*Anastrepha*, *Rhagoletis*). A dental sclerite is present in *Ceratitis* and other Dacinae but there is no dental sclerite in Trypetinae (*Anastrepha*, *Rhagoletis*). The neck and dental sclerite can be observed under a compound microscope (Figure 46, Figure 61 and Figure 62).

A lateral lip of the oral opening, apparently a single structure but usually deeply invaginated to give the appearance of being two adjacent lips (inner (medial, lateral lip) and outer (lateral, lateral lip)), is present

in the SEM images of nearly all tephritid larvae described to date but varies in extent (Figure 63 and Figure 64). Lateral to the outer lateral lip is a series of elongate ridges called the oral ridges, which may funnel liquids into the mouth during feeding. Oral ridges occur in larvae of all fruit-infesting tephritids, but they vary in number and their edges may be entire, serrate, scalloped or fringed (Figure 65, Figure 66 and Figure 67). Details of these features are best observed with an SEM or with a compound microscope as described in section 4.2.1.1.

A single series of accessory plates at the lateral margins of the oral ridges is present in most species of *Ceratitis*. Accessory plates are also present in *Bactrocera*, *Dacus* and *Anastrepha*, although their specific shapes, numbers and positions vary among genera (Figure 65, Figure 66 and Figure 67). Accessory plates are absent in *Rhagoletis*. Details are best observed with an SEM.

Anterior spiracles are located dorsolaterally on the first thoracic segment. They have an internal trunk that flares apically to one or more external rows of tubules that are short with a rounded top bearing a thin slit to allow passage of air. Individual tubules are very similar among all fruit fly larvae. However, the number of tubules, their arrangement and the overall dimensions of the spiracles may be useful in diagnosing some fruit fly species. The apical row of tubules in *Ceratitis* and other Dacinae in profile are typically fan-shaped with a flat or convex top, compared with *Anastrepha* in which the row or rows of tubules are distinctly bilobed. The anterior spiracles should be observed on cleared specimens on slides under a light microscope (Figure 68 and Figure 69).

The last larval abdominal segment has a pair of posterior spiracles located posterodorsally (Figure 70) and anal lobes located ventrally. In the Dacinae (including *Ceratitis*), a caudal ridge is present on the tubercle in the area between the posterior spiracles and anal lobe. Presence of a caudal ridge can be used to separate the subfamily Dacinae from Trypetinae, in which it is absent (Figure 71 and Figure 72). The caudal ridge is usually apparent in dorsal, caudal and lateral views, although it may be easier to see from some angles than others. The caudal ridge can be observed using either a dissecting microscope with high resolution or an SEM.

Some Dacinae have a thin, dark, sclerotized line below the caudal ridges that is visible under a dissecting microscope but not under an SEM. It is known to occur in numerous *Zeugodacus* species (Figure 73). It has not been observed in any *Ceratitis* larvae described to date.

Live, mature third instars of Dacinae display skipping (jumping) behaviour. The larva curls into a ring shape and attaches its mouthhooks to its caudal segment. When it flexes the body muscles and releases the attachment of the mouthhooks, the larva springs several centimetres into the air. This behaviour presumably is a method to escape predators. Trypetine larvae do not display this behaviour.

4.2.3 Characters to identify third instars of *Ceratitis capitata*

Useful diagnostic features given in Steck and Ekesi (2015) and by G.J. Steck (personal communication, 11 June 2021) are included in Table 3. If all of the character states in Table 3 are observed, the insect is identified as *C. capitata* for routine screening and surveillance, but molecular analysis must be performed to complete an identification for first pest records (section 4.3.5). Steck and Ekesi (2015) stated that "*C. capitata* larvae can be separated from most individuals of the [FARQ] complex by the absence of oral ridge accessory plates and the presence of dorsal spinules on T3" (see Figure 65 for oral ridge). Also, the subapical tooth of the mouthhook in *C. capitata* is absent or minute when present and usually not apparent with a light microscope (occasionally also true of *C. rosa*), and the single, wide lateral lip seen in *C. capitata* (Figure 64) has not been observed in larvae of any other *Ceratitis* species described to date.

4.2.4 Characters to identify third instars of *Ceratitis cosyra*

The diagnostic features included in Table 3 for *Ceratitis cosyra* derive from Kandybina (1977). If all of the character states in Table 3 are observed, the insect is consistent with a diagnosis as *Ceratitis cosyra*, but molecular analysis should be performed to confirm that identification for a first record (section 4.3.6).

4.2.5 Characters to identify third instars of the FARQ complex

The diagnostic features outlined in Steck and Ekesi (2015) are included in Table 3. If all of the character states in Table 3 are observed, the insect is consistent with a diagnosis as *Ceratitis* FARQ complex, but molecular analysis should be performed to confirm that identification for a first record (section 4.3.7). It is generally not possible to distinguish the four species in the FARQ complex using third-instar larvae. However, Steck and Ekesi (2015) reported that, in comparison to the other three species, *C. fasciventris* specimens tend to have "smaller dimensions of the cephaloskeleton and anterior spiracle apical width, and lower counts of spiracular processes and narrowness of their bases".

Table 3. Diagnostic morphological characters of third instars of *Ceratitis* species

Character	Species					
	C. anonae	***C. capitata***	***C. cosyra***	***C. fasciventris***	***C. quilicii* (rosa R2)**	***C. rosa* (R1)**
Dorsolateral sensilla, orientation to maxillary palpus (Figure 50)	Parallel	Parallel	Parallel	Parallel	Parallel	Parallel
Preoral organ and lobes (Figure 53)	Petal-like	Petal-like	Petal-like	Petal-like	Petal-like	Petal-like
Mouthhook, subapical tooth (Figure 58 and Figure 59)	Present	Present or absent	Present	Present	Present or absent	Present
Cephaloskeleton, total length (Figure 46)	1.16–1.23 mm	1.06–1.11 mm	n/a	0.89–1.14 mm	1.14–1.34 mm	0.99–1.26 mm
Lateral lips, number and width (Figure 63 and Figure 64)	2, narrow	1, wide	2, narrow	2, narrow	2, narrow	2, narrow
Oral ridges, number (Figure 65 and Figure 66)	10–11	8–12	10–12	9–10	8–12	8–12
Oral ridge margins (Figure 65 and Figure 66)	Scalloped	Scalloped (rarely entire)	Scalloped	Scalloped	Scalloped	Scalloped
Accessory plates, number, size and dentition (Figure 65 and Figure 66)	8–12, well-developed, some scalloped	Absent	9–13, short linear and irregular nubs, not scalloped	3–8, small or nubs	Geographically variable: absent or nubs to 4–7 well-developed, some scalloped	7–11, well-developed, some scalloped
Dorsal spinules (Figure 49)	Present on T1–T2	Present on T1–T3 (rarely A1)	Present on T1–T3	Present on T1–T2	Present on T1–T2	Present on T1–T2
Anterior spiracle, number of tubules* (Figure 68)	10–13	9–12	11–12	9–12	10–13	8–15
Anterior spiracle, apical width (Figure 68)	0.19–0.24 mm	0.16–0.19 mm	n/a	0.14–0.17 mm	0.18–0.24 mm	0.16–0.21 mm
Caudal ridge (Figure 71)	Present	Present	Present	Present	Present	Present

Notes: *Ranges are reported from Steck and Ekesi (2015) and represent the range for species based on most commonly found values. Outlier specimens with values outside of ranges could exist (G.J. Steck, personal communication, 2022) and are reported in other sources (e.g. White and Elson-Harris, 1992).

A1, first abdominal segment; n/a, data not yet available; T1, T2, T3, first, second and third thoracic segments.

Steck, G.J. & Ekesi, S. 2015. Description of third-instar larvae of *Ceratitis fasciventris*, *C. anonae*, *C. rosa* (FAR complex) and *C. capitata* (Diptera, Tephritidae). *ZooKeys*, 540: 443–466.

White, I.M. & Elson-Harris, M.M. 1992. *Fruit flies of economic significance: their identification and bionomics*. Wallingford, UK, CABI. 601 pp.

4.3 Molecular identification of *Ceratitis* species

Methods for molecular identification have been published for several *Ceratitis* species (Barr *et al.*, 2006, 2012; Virgilio *et al.*, 2017). Additional studies have investigated the population genetics of *C. capitata* (section 4) and the molecular evolution of the group (Barr and McPheron, 2006; Virgilio *et al.*, 2008; Barr and Wiegmann, 2009; Erbout *et al.*, 2011; Zhang *et al.*, 2021). The current protocol includes those molecular methods that have been applied to specimen identification of specific pests for which diagnostic sensitivity and specificity has been measured. Additional molecular datasets such as DNA sequence records from phylogenetic studies could be valuable in supporting information for identifications but are not yet described as diagnostic methods.

Species identification based on comparison of DNA sequences of a fragment of the *COI* gene of animals is commonly referred to as DNA barcoding (Hebert *et al.*, 2003; Floyd *et al.*, 2010). This diagnostic technique has been applied to tephritid fruit flies in several studies to demonstrate the performance of the technology (Armstrong and Ball, 2005; Virgilio *et al.*, 2010; Jiang *et al.*, 2014). Development of DNA barcode data into an identification method for specific pests has been examined for *C. capitata* (Barr *et al.*, 2012) and *C. cosyra* (Virgilio *et al.*, 2017). However, the DNA barcoding method is not sufficient to complete species-level identifications for members of the FARQ species complex: *C. anonae*, *C. fasciventris*, *C. rosa* and *C. quilicii* (Virgilio *et al.*, 2010; Barr *et al.*, 2012; Virgilio *et al.*, 2012, 2019; Zhang *et al.*, 2021).

In the case of *C. capitata*, the method does not separate *C. capitata* from its sister species, *C. caetrata*. As a result, identification of a specimen as *C. capitata* using DNA barcoding is dependent on considering a reduced taxonomic scope in the diagnosis process. This reduced scope is achieved by excluding *C. caetrata* as a possible outcome in the diagnosis, where possible, on the basis of its restricted host range, which includes indigenous wild fruit but not commercially grown fruit, and its limited geographical distribution: *C. caetrata* has not been detected outside of Kenya (De Meyer, 2001; De Meyer *et al.*, 2002, 2004). The inability to separate *C. capitata* and *C. caetrata* is also true of the real-time PCR method developed for diagnosis of *C. capitata* based on *COI* gene sequence differences (described in section 4.3.5.2).

If confirmatory analysis is required to identify *C. capitata* collected in regions where it co-occurs with *C. caetrata*, then it is possible to compare amplicon lengths of a ribosomal (r)RNA target as reported by Barr *et al.* (2006). In that study, a 26 base pair (bp) size difference was observed between *C. capitata* and *C. caetrata* because of the internal transcribed spacer 1 (ITS-1) of the rRNA array (section 4.3.5.3).

Analyses of *C. cosyra* specimens using microsatellite DNA (Virgilio *et al.*, 2015) and mitochondrial DNA (Barr *et al.*, 2012; Frey *et al.*, 2013; Virgilio *et al.*, 2017) support the hypothesis of cryptic species under the name *C. cosyra*. Virgilio *et al.* (2017) distinguished at least two lineages, named *C. cosyra* group 1 and *C. cosyra* group 2. These two groups do not form one monophyletic lineage with respect to other *Ceratitis* species based on analysis of the mitochondrial *COI* gene. Of the *C. cosyra* specimens included in molecular studies, group 1 is the dominant lineage because it is reported from a greater number of specimens and from collections over a wider geographical distribution range. The DNA barcoding method can identify a fly to species *C. cosyra* group 1 or to *C. cosyra* group 2 based on high DNA sequence similarity (Virgilio *et al.*, 2017).

Phylogenetic analysis of *C. cosyra COI* DNA sequences has identified additional specimens that do not cluster into group 1 or group 2. These sequences were from specimens that either could not be confirmed to be *C. cosyra* using morphology or had pseudogene copies of the *COI* gene that preclude diagnostic analysis of the data (Barr *et al.*, 2012; Virgilio *et al.*, 2017). As summarized by Virgilio *et al.* (2017), the species limits of *C. cosyra* and potential cryptic species that look like *C. cosyra* are not yet known. Insufficient information is available to conclude that a fly is not *C. cosyra* based on dissimilarity to records reported from either group 1 or group 2.

The *COI* records for the members of the FARQ complex form a monophyletic clade with respect to other species in phylogenetic trees, indicating that identification of the FARQ complex as a group is

possible using DNA barcode data (Barr and McPheron, 2006; Virgilio *et al.*, 2008, 2019), but there are limitations to using tree-based identification methods for the data (Meier *et al.*, 2006; DeSalle and Goldstein, 2019). Reliable identification of flies to the level of the FARQ complex based on percentage divergence between *COI* sequences has not been demonstrated.

Once a fly is identified as a member of the FARQ complex based on morphology or mitochondrial DNA (barcode) data, additional analysis using comparative genomics (Zhang *et al*., 2021) or 16 microsatellite DNA markers (Virgilio *et al.*, 2013, 2019; Delatte *et al.*, 2014) can distinguish the four species. However, methods for genome analysis have not been converted into validated diagnostic methods. The microsatellite DNA technique requires comparison of PCR-amplified alleles with alleles of reference material to correctly score the size of the allele fragments and complete computational analysis of admixture coefficients to determine the fly's identity. Reference material of these species is not readily available, and the method has not been replicated in multiple laboratories yet. Consequently, these methods are not provided in detail in the current protocol.

4.3.1 Sample preservation, preparation and DNA extraction for molecular tests

Boykin *et al.* (2014) and Ball and Armstrong (2008) provide protocols for DNA extraction using commercial kits that are useful because small amounts of starting material, such as one fruit fly leg, can give enough DNA yield and quality for PCR. The methods used to preserve fruit flies for morphological and molecular examination are not the same. Ethanol is a common preservative for fruit fly DNA. Although fruit fly specimens can be preserved in ≥95% ethanol at −20 °C or colder for long-term storage, percentages of ethanol above 70% can make larvae more difficult to dissect. Preparation of larvae for morphological examination includes a boiling step (section 4.2.1) before storage. This boiling step is compatible with molecular study but not required to process larvae in molecular analyses. The boiling step is recommended if a voucher of the specimen is to be retained for morphological examination. It is possible to soak larvae in DNA extraction lysis buffers overnight to isolate nucleic acids from specimens, and then use the larvae in slide mounting. These buffer-soaked larvae, however, are not appropriate for SEM examination.

In cases where molecular and morphological methods are to be used, it is therefore recommended that a portion of the larva (such as the fourth or fifth abdominal segment) be excised (see section 4.2.1), or a hind leg be removed (see beginning of section 4), and stored in ethanol for DNA extraction. The remaining specimen can be prepared for morphological work. It is important to ensure that the remaining legs of adults are available for morphological examination as the characters present on the legs are used to identify *Ceratitis* species. Further examples of methods are provided by Plant Health Australia (2016).

4.3.2 Controls for molecular tests

For the test result to be considered reliable, appropriate controls should be considered for each series of nucleic acid extractions and PCR amplifications of the target pest. As a minimum, a positive nucleic acid control, a negative amplification control (no template control), and a negative extraction control should be used for a PCR test used to conduct DNA barcoding or for a real-time PCR test.

Positive nucleic acid control. This control is used to monitor the efficiency of the method used for the test (apart from the extraction). Pre-prepared (stored) genomic target DNA may be used.

Negative amplification control (no template control). This control is necessary to rule out false positives resulting from contamination with other genetic material during the preparation of the reaction mixture. PCR-grade water that was used to prepare the reaction mixture is added in place of template DNA.

Negative extraction control. This control is used to monitor contamination during nucleic acid extraction. This requires extraction blanks to be processed alongside the samples to be tested.

4.3.3 PCR amplification for DNA barcoding flies in the genus *Ceratitis*

DNA barcoding methods for *Ceratitis* species have been reported by Barr *et al.* (2012) and Virgilio *et al.* (2010, 2012). The Barr *et al.* (2012) study specifically addressed the use of the method for identification of *C. capitata*. In that study, primer selection impacted amplification of alternate copies of the target for several species, including specimens of *C. capitata*. The Folmer *et al.* (1994) and Simon *et al.* (1994) primer pairs used by Barr *et al.* (2012) are included here to provide two options for completing DNA barcoding of the pest. Amplification can be accomplished using the reagents and cycling parameters presented in Table 4.

The oligonucleotide primers used from Folmer *et al.* (1994) are:

LCO-1490 (forward): 5′-GGT CAA CAA ATC ATA AAG ATA TTG G-3′

HCO-2198 (reverse): 5′-TAA ACT TCA GGG TGA CCA AAA AAT CA-3′

The oligonucleotide primers used from Simon *et al.* (1994) are:

TY-J-1460 (forward): 5′- TAC AAT TTA TCG CCT AAA CTT CAG CC-3′

C1-N-2191 (reverse): 5′- CCC GGT AAA ATT AAA ATA TAA ACT TC-3′

Table 4. Master mix composition, thermal cycling parameters and amplicons for PCR to amplify *COI* barcode from *Ceratitis capitata*

Reagents	Final concentration
PCR-grade water	–[†]
PCR buffer	1×
$MgCl_2$	2.5 mM
dNTPs	200 µM of each
Primer (forward)	0.2 µM
Primer (reverse)	0.2 µM
DNA polymerase	0.025 U/µL
DNA sample	1 µL
Cycling parameters	
Initial denaturation	94 °C for 3 min
Number of cycles	35
Denaturation	94 °C for 20 s
Annealing	50 °C for 20 s
Elongation	72 °C for 30 s
Final elongation	72 °C for 5 min
Expected amplicons	
Size	c. 709 bp (Folmer *et al.* primer set) c. 775 bp (Simon *et al.* primer set)

Notes: [†] For a final reaction volume of 25 µL or 50 µL.

bp, base pairs; c., approximately; PCR, polymerase chain reaction.

Folmer, O., Black, M., Hoeh, W., Lutz, R. & Vrijenhoek, R. 1994. DNA primers for amplification of mitochondrial cytochrome c oxidase subunit I from diverse metazoan invertebrates. *Molecular Marine Biology and Biotechnology*, 3: 294–299.

Simon, C., Frati, F., Beckenbach, A., Crespi, B., Liu, H. & Flook, P. 1994. Evolution, weighting, and phylogenetic utility of mitochondrial gene sequences and a compilation of conserved polymerase chain reaction primers. *Annals of the Entomological Society of America*, 87: 651–701.

If the negative controls generate amplicons, then the results are not valid. If the positive control fails to generate the expected product, the results are not valid. Only sequences of PCR products from good test runs are considered for the diagnosis.

4.3.4 DNA sequence editing and quality control for DNA barcoding data

The DNA sequencing of PCR products should be carried out using each PCR primer to generate two DNA sequence reads in alternate directions. In addition to the output of base sequence data reported as text, the chromatogram and Phred scores used to determine base calls should also be examined during the editing process and stored with records. The two sequences should be aligned to create a consensus sequence and then visually examined to identify conflicting information. Chromatograms should be edited to resolve conflicting signals. Sites that are not corroborated by data in both sequences because of differences in lengths should be removed or assigned as an ambiguous base (i.e. N = A, C, T or G). If multiple peaks are observed at a nucleotide site in both the forward-primed and reverse-primed sequences, then the site should be assigned as an ambiguous base (i.e. N) in the consensus sequence. If conflict is the result of ambiguity at a site because of two sequences and each has a high Phred score (>30), then the site should be assigned as an ambiguous base (i.e. N). Diagnosis should only be performed on edited sequences having less than 0.5% ambiguous bases. The final sequence length of the query sequence should be at least 500 bp for data interpretation. Additional information on data-editing processes is available in EPPO (2016).

Once a consensus sequence has been generated, the data should be queried against records of the International Nucleotide Sequence Database Collaboration, which comprises the DNA DataBank of Japan, the European Nucleotide Archive, and GenBank at the National Center for Biotechnology Information (NCBI). The query can be performed using the default setting for blastn searches in the Basic Local Alignment Search Tool (BLAST) of NCBI: https://blast.ncbi.nlm.nih.gov/Blast.cgi. The best sequence match between the query consensus and the database (i.e. the match with the highest Max Score) should be a species in the genus *Ceratitis*. If the query is a best match to a *Ceratitis* record, then the consensus sequence is appropriate for further DNA barcode comparison and interpretation in the protocol (section 4.3.5.1, section 4.3.6.1 and section 4.3.7.1). If the query is not a best match to a *Ceratitis* record, then the consensus sequence is not appropriate for further DNA barcode comparison because it could be a contaminant, a pseudogene, a *Ceratitis* species not previously reported, or a species outside the scope of the protocol.

Before completing a diagnosis, the query nucleotide sequence should be translated into an amino acid sequence and compared to the amino acid translation of *Ceratitis* records (section 4.3.5, section 4.3.6 or section 4.3.7) to detect evidence of premature stop codons and reading-frame shifts (frameshifts) that suggest a pseudogene has been amplified and sequenced. Paralogous copies of *COI* such as pseudogenes should not be interpreted using the DNA barcoding methods included in this protocol. However, it can be difficult to detect pseudogenes and other paralogs of the *COI* gene because DNA barcode records can lack evidence of insertions or deletion in the nucleotide alignment and disruptions to amino acid translation codes (Buhay, 2009). In addition to detecting frameshift mutations, the protocol includes steps to assist in paralogous copy recognition based on high rates of ambiguous calls (i.e. conflicting calls of multiple peaks) and high mutation rates for a specimen observed as a long branch in the clade of a phylogenetic tree. Paralogous copies of *COI* and other mitochondrial genes have been reported for *Ceratitis* species, including *C. capitata* and *C. cosyra* (Barr *et al.*, 2006, 2012) and other fruit flies (e.g. Blacket, Semeraro and Malipatil, 2012). It is possible for paralogous copies of a mitochondrial gene to be preferentially amplified instead of the orthologous copy during PCR in *Ceratitis* (Barr *et al.*, 2006, Barr and McPheron 2006). Virgilio *et al.* (2012) included a record for *C. capitata* (DQ011888) that is inconsistent with estimated intraspecific variation for the species and is possibly a misidentified specimen or a paralogous copy of the *COI* gene.

4.3.5 Molecular tests for *Ceratitis capitata*

Species identification can be completed for *C. capitata* using DNA barcoding (section 4.3.5.1), assuming *C. caetrata* can be excluded as a possible identification based on its host use and limited

distribution. If it is possible that *C. caetrata* is present in the same trap, host or pathway as *C. capitata*, then an additional test for amplicon size of a ribosomal (r)DNA PCR target can be performed to distinguish the two species (section 4.3.5.3). A real-time PCR test (section 4.3.5.2) may identify *C. capitata* in pathways and areas where its presence is expected, but DNA barcoding should be used to confirm new records if based on molecular data.

4.3.5.1 DNA barcoding to identify Ceratitis capitata

Barr *et al.* (2012) demonstrated that an uncorrected p-distance measure of 2% was appropriate to capture intraspecific variation and that a barcode gap existed between *C. capitata* and the close relative *Ceratitis pinax*. After exclusion of an atypical sequence (DQ011888), Virgilio *et al.* (2012) also reported an expected divergence of 2% using p-distance or Kimura two-parameter distance. In both studies, the next most similar species (*Ceratitis catoirii*, *Ceratitis malgassa* and *C. pinax*) were greater than 5% distant from the *C. capitata* and *C. caetrata* DNA records. Barr *et al.* (2012) also examined the dataset using DNA character states and determined that a clade including *C. capitata* and *C. caetrata* can be diagnosed from other species. The DNA barcoding method described in this protocol to identify *C. capitata* is based on these studies and describes one reliable approach to diagnose *C. capitata* without reliance on databases that can change over time. The PCR method for amplification of the *COI* target is provided in section 4.3.3.

Before analysis and interpretation, the quality of the query DNA sequence data should be confirmed using the recommendations of section 4.3.4 regarding the number of ambiguous bases, overall data quality, and the need to confirm a match to a *Ceratitis* record on a public server.

If quality conditions are met (see section 4.3.4), the consensus sequence of the query should be aligned to the *COI* records reported in Barr *et al.* (2012) and available from GenBank as PopSet407912263. This can be accomplished using an algorithm such as CLUSTAL and visual examination of alignment.

The alignment can be used to generate a phylogenetic tree based on characters (e.g. maximum parsimony, maximum likelihood criteria). This provides an assessment of character-based similarities between the query and the records in the alignment. The query sequence is interpreted to be a *C. capitata* sequence if the query sequence is in a clade that consists exclusively of *C. capitata* and *C. caetrata* sequences. If the query sequence does not form a clade that consists exclusively of *C. capitata* and *C. caetrata* sequences in the tree, this is evidence in support of the sequence being a species other than *C. capitata* or *C. caetrata*. It is possible for paralogous copies of *COI* to form a clade with reference sequences and complicate interpretation. A comparison of the query records to reported genetic-distance values between orthologous copies of the pest can assist in detecting possible pseudogenes or confirming the tree-based interpretation.

Next, to confirm a positive identification from the phylogenetic-tree result, the edited sequence should be aligned to three reference sequences: GenBank accessions GQ154188 (*C. capitata*), GQ154186 (*C. caetrata*) and GQ154194 (*C. catoirii*) from reference specimens at the Royal Museum for Central Africa. The pairwise, uncorrected percent differences among the four sequences should be computed and the results used to determine if the follow conditions are true:

(1) The distance between the query sequence and GQ154188 (*C. capitata*) record is less than 2%.

(2) The distance between the query sequence and GQ154186 (*C. caetrata*) record is less than 2%.

(3) The distance between the query sequence and GQ154194 (*C. catoirii*) record is greater than 5%.

If these three conditions are true for genetic-distance measures, and the query sequence forms a clade that consists exclusively of *C. capitata* and *C. caetrata* sequences in the phylogenetic tree, then the query is identified as *C. capitata*.

If the query sequence is greater than 5% divergent from the *C. capitata* and *C. caetrata* reference records, and the query sequence does not form a clade consisting exclusively of *C. capitata* and *C. caetrata* sequences in the phylogenetic tree, then the query specimen is not consistent with

C. capitata. Identification as *C. cosyra* (section 4.3.6) or a FARQ complex species (section 4.3.7) can be examined using this protocol.

If the results do not match either of these two outcomes, then the specimen cannot be identified. In this situation, the genetic results are inconsistent with genetic-distance estimates from prior datasets. It is possible that the sequence is a paralogous copy of the *COI* gene.

4.3.5.2 Real-time PCR to identify Ceratitis capitata

This real-time PCR, developed by Dhami *et al.* (2016), is designed to amplify a 97 bp fragment of the *COI* gene from *C. capitata* based on *in silico* comparison of 314 barcode records. The method uses TaqMan probe chemistry and was developed and validated using a single commercial real-time PCR reagent mixture. Validation measurements reported in Dhami *et al.* (2016) are for analytical sensitivity, repeatability and reproducibility. In addition to the *in silico* comparisons, diagnostic sensitivity was assessed experimentally using 20 *C. capitata* specimens and diagnostic specificity was assessed using 90 flies in other genera (*Bactrocera*, *Dacus* and *Zeugodacus*) and 5 *Ceratitis* flies: 3 *C. caetrata*, 1 *C. cosyra* and 1 *C. rosa*. The *C. caetrata* specimens did cross-react in the real-time method, but the other species assessed did not cross-react.

Dhami *et al.* (2016) reported that a TaqMan 18S internal control may be used with this method to demonstrate that failure to amplify the *C. capitata* target is not the result of poor sample quality.

Diagnosis of flies based on a real-time PCR is not sufficient to complete accurate species identification under all circumstances. Diagnostic specificity within the genus *Ceratitis* has been demonstrated using *in silico* comparisons, but real-time PCR to check for cross-reaction under laboratory conditions against all *Ceratitis* pest species has not been performed. However, a diagnosis to *C. capitata* that is based solely on a real-time PCR result could be appropriate when screening for the pest where its presence is expected and where other *Ceratitis* species that could be mistaken for the pest are absent. Morphological identification of an adult or DNA barcoding analysis of a larva should be performed to complete the identification of a fly when the diagnosis is intended to confirm a new record of pest presence.

The oligonucleotide primers and probes used are:

Ccap2F (forward primer): 5′-GCT GTA AAT TTT ATC ACA ACA-3′

Ccap3R (reverse primer): 5′-GTG CAG TAA GAA CTA CTG-3′

Ccap2P (hydrolysis probe): 5′-(Quasar 670/Cal Red)-CGG AAT TTC ATT CGA CCG AAT ACC T–(BHQ-1)-3′

The master mix and PCR cycling parameters are described in Table 5.

Table 5. Master mix composition, thermal cycling parameters and amplicons for real-time PCR to identify *Ceratitis capitata*

Reagents	Final concentration
PCR-grade water	–†
master mix*	1×
BSA (10mg/ml)	0.05 µg/µL
Primer (forward)	0.5 µM
Primer (reverse)	0.5 µM
Probe	0.2 µM
DNA polymerase	(in master mix)
DNA sample	1–20 ng
Cycling parameters	
Initial denaturation	95 °C for 2 min
Number of cycles	35
Denaturation	95 °C for 10 s
Annealing	58 °C for 60 s
Expected amplicons	
Size	97 bp

Notes: * Master mix containing dNTPs, polymerase, $MgCl_2$, buffer or stabilizers, normalization dyes.

† For a final reaction volume of 10 µL.

bp, base pairs; BSA, bovine serum albumin; PCR, polymerase chain reaction.

If the negative controls generate amplicons, then the results are not valid. If the positive control fails to generate the expected product within the 35 cycles, then the results are not valid. The product of the positive control must generate a sigmoidal growth curve to be interpreted as a positive result. The experimental specimens are identified as *C. capitata* (or *C. caetrata*) only when a product is generated within the 35 cycles and has a sigmoidal growth curve.

Failure to generate a real-time PCR product consistent with the *C. capitata* target is not sufficient to determine that the specimen is not *C. capitata*, as it is possible that the nucleic acid sample of the specimen was not appropriate (e.g. degraded nucleic acids) for real-time PCR. In these circumstances, an additional PCR-based test of the extracted DNA, such as the conventional PCR to amplify *COI* described in section 4.3.3, must therefore also be performed to confirm that nucleic acid quality and quantity did not impact the result. Dhami *et al.* (2016) demonstrated that commercially available eukaryotic 18S real-time PCR control kits can also be used to confirm suitability of the extraction for diagnosis of *C. capitata*. The *COI* conventional PCR and 18S real-time PCR options must also include positive and negative controls. The positive controls and experimental samples for the 18S real-time PCR are only positive if they generate a product within 35 cycles and have a sigmoidal growth curve. The relative sensitivity of the *COI* conventional PCR and the *COI* and 18S real-time PCR have not been reported.

4.3.5.3 PCR of rDNA to distinguish Ceratitis capitata *and* Ceratitis caetrata

Barr *et al.* (2006) demonstrated a size difference for the ITS-1 rDNA located in the rRNA gene array between *C. capitata* and *C. caetrata*. Using the primers report by Douglas and Haymer (2001), the ITS-1 locus was amplified from five species: *C. anonae*, *C. caetrata*, *C. capitata*, C. *fasciventris* and *C. rosa*. The specimens of *C. capitata* and *C. caetrata* generated distinct sizes that differed by 26 bases. The amplicon sizes predicted *in silico* were 1 028 bp for *C. caetrata* (AY782168.1) and 1 002 for *C. capitata* (AF307848.1). Repeating the procedure on a series of specimens for each species generated consistent band-size differences in species (Barr *et al.*, 2006). This method provides diagnostic information to separate *C. capitata* and *C. caetrata*, but additional information from morphology or DNA analysis is

required to determine whether the query fly is one of the two species. Subsequent work by Virgilio *et al.* (2008) re-examined ITS-1 from a larger collection of *C. anonae*, C. *fasciventris* and *C. rosa* specimens and reported sharing of size variants among those species.

The oligonucleotide primers used by Douglas and Haymer (2001) are:

ITS1-F5 (forward): 5′- CAC GGT TGT TTC GCA AAA GTT -3′

ITS1-B9 (reverse): 5′- TGC AGT TCA CAC GAT GAC GCA C -3′

The master mix and PCR cycling parameters are described in Table 6.

Table 6. Master mix composition, thermal cycling parameters and amplicons for PCR to amplify ITS-1 from *Ceratitis capitata*

Reagents	**Final concentration**
PCR-grade water	–†
PCR buffer	1×
$MgCl_2$	2.5 mM
dNTPs	200 µM of each
Primer (forward)	0.05 µM
Primer (reverse)	0.05 µM
DNA polymerase	0.025 U/µL
DNA sample	1 µL
Cycling parameters	
Initial denaturation	94 °C for 3 min
Number of cycles (round 1)	10
Denaturation	94 °C for 60 s
Annealing	60 °C for 60 s
Elongation	72 °C for 60 s
Number of cycles (round 2)	10
Denaturation	94 °C for 60 s
Annealing	58 °C for 60 s
Elongation	72 °C for 60 s
Number of cycles (round 3)	10
Denaturation	94 °C for 60 s
Annealing	57 °C for 60 s
Elongation	72 °C for 60 s
Final elongation	72 °C for 10 min
Expected amplicons	
Size	1 002 bp or 1 028 bp

Notes: † For a final reaction volume of 25 µL or 50 µL.

bp, base pairs; PCR, polymerase chain reaction.

If the negative controls generate amplicons, then the results are not valid. If the positive control fails to generate the expected product, then the results are not valid. Amplicon size differences can be scored on 1.4% agarose gels. The results for the query fly should be compared to those of a known *C. capitata* and *C. caetrata* to compare amplicon size or to one of the species and a molecular ladder that can discriminate the band sizes in the range.

4.3.6 Molecular tests for *Ceratitis cosyra*

The name *C. cosyra* currently includes multiple cryptic species (Virgilio *et al.*, 2017). Molecular identification can be completed for two lineages within the species referred to as *C. cosyra* group 1 and *C. cosyra* group 2 using DNA barcoding (section 4.3.6.1).

4.3.6.1 DNA barcoding for Ceratitis cosyra

DNA barcoding methods for *C. cosyra* have been reported by Barr *et al.* (2012) and Virgilio *et al.* (2017). In the Barr *et al.* (2012) study, pseudogene copies were reported in the species. The Virgilio *et al.* (2017) study demonstrated that using either an uncorrected p-distance or Kimura two-parameter distance of 2% for similarity match was successful in identifying specimens to the *C. cosyra* group 1 and *C. cosyra* group 2 clades. The Barr *et al.* (2012) study included group 1 specimens and generated similar distance measures of genetic diversity within the species; the study did not include group 2 specimens.

Identification to either *C. cosyra* group is based on a high similarity match between *COI* barcode sequences. It is not possible to conclude that a query fly is not *C. cosyra* based on high dissimilarity between the query and *C. cosyra COI* sequences. This is because the cryptic species limits are unknown and highly divergent copies of *COI* have been reported from *C. cosyra* specimens. The PCR method for amplification of the *COI* target is provided in section 4.3.3.

Before analysis and interpretation, the quality of the query DNA sequence data should be confirmed using the recommendations of section 4.3.4 regarding number of ambiguous bases, overall data quality, and the need to confirm a match to a *Ceratitis* record on a public server.

If quality conditions are met (see section 4.3.4), the consensus sequence of the query should be aligned to the *COI* records reported by Virgilio *et al.* (2017) and available at this link: dx.doi.org/10.5883/DS-COSYRA. The alignment can be used to generate a phylogenetic tree based on characters (e.g. maximum parsimony, maximum likelihood criteria) to assess character-based similarities between the query and the records in the alignment.

The query sequence is interpreted to be a *C. cosyra* sequence if the query sequence is in a clade that consists exclusively of *C. cosyra* sequences. If the query sequence does not form a clade that consists exclusively of *C. cosyra* sequences in the tree, this should not be interpreted as evidence that the sequence is *not C. cosyra*, because the species appears to form polyphyletic lineages in trees and might be a cryptic species (Virgilio *et al.*, 2017). It is also possible for paralogous copies of *COI* to form a clade with reference sequences and complicate interpretation. A comparison of the query records to reported genetic-distance values between orthologous copies of the pest can assist in detecting possible pseudogenes or confirming the tree-based interpretation.

Next, to confirm a positive identification in the phylogenetic tree result, the edited sequence should be aligned to a *C. cosyra* group 1 record (GenBank accession GQ154202) and *C. cosyra* group 2 record (GenBank accession GQ154204) from reference specimens at the Royal Museum for Central Africa. The pairwise, uncorrected percent differences among the three sequences should be computed and the results used to determine the identification.

If the distance between the query sequence and the GQ154202 (*C. cosyra* group 1) record is less than 2%, and the query sequence forms a clade that consists exclusively of *C. cosyra* sequences in the phylogenetic tree, then the query fly is identified as *C. cosyra* group 1.

If the distance between the query sequence and the GQ154204 (*C. cosyra* group 2) record is less than 2%, and the query sequence forms a clade that consists exclusively of *C. cosyra* sequences in the phylogenetic tree, then the query fly is identified as *C. cosyra* group 2.

If the results do not match either of these two outcomes, then the specimen cannot be identified. In this situation, the genetic results are inconsistent with genetic-distance estimates from prior datasets. It is possible that the sequence is a paralogous copy of the *COI* gene.

4.3.7 Molecular tests for the FARQ complex

Molecular methods can diagnose a specimen to the level of the FARQ complex using DNA barcoding (section 4.3.7.1). As explained at the beginning of section 4.3, molecular identification of FARQ complex specimens to the level of species (i.e. *C. anonae*, *C. fasciventris*, *C. rosa* and *C. quilicii*) requires microsatellite or genomic DNA examination but details for the associated procedure are not provided in this protocol. Identification of a fly to the FARQ complex is a prerequisite for subsequent microsatellite DNA diagnosis.

4.3.7.1 DNA barcoding the FARQ complex

The species *C. anonae*, *C. fasciventris*, *C. rosa* and *C. quilicii* form a monophyletic clade in phylogenetic trees constructed using *COI* data, but the species are polyphyletic within the clade (Barr and McPheron, 2006; Virgilio *et al.*, 2008, 2019; Zhang *et al.*, 2021). The *COI* genetic-distance estimates between two FARQ complex specimens and between a FARQ complex specimen and a non-FARQ complex *Ceratitis* specimen can be similar and near 2.5% for some comparisons (Barr *et al.*, 2012). A threshold value for identification of the FARQ complex based on genetic distances has not been reported for diagnostic application. Molecular identification to the FARQ complex level using DNA barcoding depends on a comparison of the query sequence in a tree-based identification and the analysis of genetic-distance measures to confirm that diversity is within expected levels. The PCR method for amplifying the *COI* target is provided in section 4.3.3.

If quality conditions are met (section 4.3.4), the consensus sequence of the query should be aligned to the *COI* records reported in both Barr *et al.* (2012) and Virgilio *et al.* (2010). These are stored in GenBank as PopSet407912263 and PopSet339262093, respectively. The two datasets and the query sequence can be aligned using an algorithm such as CLUSTAL and visual examination of alignment. The alignment can be used to generate a phylogenetic tree based on characters (e.g. maximum parsimony, maximum likelihood criteria) to assess character-based similarities between the query and the records in the alignment.

The query sequence is interpreted to be a FARQ complex sequence if the query sequence is in a clade that consists exclusively of sequences of FARQ complex species. If the query sequence does not form a clade that consists exclusively of FARQ complex sequences in the tree, this is evidence in support of the sequence being a species other than those in the FARQ complex. It is also possible for paralogous copies of *COI* to form a clade with reference sequences and complicate interpretation. A comparison of the query records to reported genetic-distance values between orthologous copies of the pest can assist in detecting possible pseudogenes or confirming the tree-based interpretation.

To confirm that genetic distances between the query and the FARQ complex sequences are consistent with prior estimates of genetic variation, the query sequence should be aligned to the following two FARQ complex records from reference specimens at the Royal Museum for Central Africa: *C. anonae* (GenBank accession GQ154176) and *C. rosa* (GenBank GQ154252). The pairwise, uncorrected percent difference between the query and the two FARQ complex records should be computed and the results used to determine the identification.

If the distance between the query sequence and *C. anonae* (GQ154176) is less than 2% and the distance between the query sequence and *C. rosa* (GQ154252) is less than 2%, then the query fly is identified as FARQ complex.

If the phylogenetic tree results and genetic distance do not match the expected outcomes for the FARQ complex, then the query fly cannot be identified. In this situation, the genetic results are inconsistent with genetic-distance estimates from prior datasets. It is possible that the sequence is a paralogous copy of the *COI* gene.

5. Records

Records and evidence should be retained as described in section 2.5 of ISPM 27 (*Diagnostic protocols for regulated pests*).

In cases where other contracting parties may be adversely affected by the diagnosis, the records and evidence of the results of the diagnosis (in particular, preserved or slide-mounted specimens, photographs of distinctive taxonomic structures, DNA extracts and photographs of gels, DNA sequence files with chromatograms, aligned DNA sequences, as appropriate) should be kept for at least one year in a manner that ensures traceability.

6. Contact points for further information

Further information on this protocol can be obtained from:

USDA-APHIS, Moore Air Base, Bldg. S-6414, 22675 N. Moorefield Rd., Edinburg, TX 78541, United States of America (Norman Benjamin Barr; email: Norman.B.Barr@aphis.usda.gov).

Florida Dept of Agriculture and Consumer Services, Division of Plant Industry, 1911 SW 34th Street, Gainesville, FL 32608, United States of America (Gary J. Steck; email: G.Steck@FDACS.gov).

Royal Museum for Central Africa, Entomology Section, Leuvensesteenweg 13, B-3080 Tervuren, Belgium (Marc De Meyer; email: demeyer@africamuseum.be; and Massimiliano Virgilio; email: massimiliano.virgilio@africamuseum.be).

A request for a revision to a diagnostic protocol may be submitted by national plant protection organizations (NPPOs), regional plant protection organizations (RPPOs) or Commission on Phytosanitary Measures (CPM) subsidiary bodies through the IPPC Secretariat (ippc@fao.org), who will forward it to the Technical Panel on Diagnostic Protocols (TPDP).

7. Acknowledgements

The first draft of this protocol was written by Marc De Meyer (Royal Museum for Central Africa, Belgium (see preceding section)), Massimiliano Virgilio (Royal Museum for Central Africa, Belgium (see preceding section)), Norman Barr (USDA-APHIS, United States of America (see preceding section)) and Gary Steck (Florida Department of Agriculture and Consumer Services, United States of America (see preceding section)). In addition, the following experts contributed to the development of this protocol: Nader Elbadry (Central Administration of Plant Quarantine, Egypt), Stephen Gaimari (Plant Pest Diagnostics Center, California Department of Food & Agriculture, United States of America) and Angel Ramirez-Suarez (Servicio Nacional de Sanidad, Inocuidad y Calidad Agroalimentaria (SENASICA), Mexico).

8. References

The present annex may refer to ISPMs. ISPMs are available on the International Phytosanitary Portal (IPP) at https://www.ippc.int/core-activities/standards-setting/ispms.

Armstrong, K.F. & Ball, S.L. 2005. DNA barcodes for biosecurity: invasive species identification. *Philosophical Transactions of the Royal Society B*, 360: 1813–1823.

Ball, S.L. & Armstrong, K.F. 2008. Rapid, one-step DNA extraction for insect pest identification by using DNA barcodes. *Journal of Economic Entomology*, 101: 523–532.

Barr, N.B. 2009. Pathway analysis of *Ceratitis capitata* (Diptera: Tephritidae) using mitochondrial DNA. *Journal of Economic Entomology*, 102: 401–411.

Barr, N.B., Copeland, R.S., De Meyer, M., Masiga, D., Kibogo, H.G., Billah, M.K., Osir, E., Wharton, R.A. & McPheron, B.A. 2006. Molecular diagnostics of economically important *Ceratitis* fruit fly species (Diptera: Tephritidae) in Africa using PCR and RFLP analyses. *Bulletin of Entomological Research*, 96: 505–521.

Barr, N.B., Islam, M.S., De Meyer, M. & McPheron, B.A. 2012. Molecular identification of *Ceratitis capitata* (Diptera: Tephritidae) using DNA sequences of the *COI* barcode region. *Annals of the Entomological Society of America*, 105: 339–350.

Barr, N.B. & McPheron, B.A. 2006. Molecular phylogenetics of the genus *Ceratitis* (Diptera: Tephritidae). *Molecular Phylogenetics and Evolution*, 38: 216–230.

Barr, N.B. & Wiegmann, B.M. 2009. Phylogenetic relationships of *Ceratitis* fruit flies inferred from nuclear CAD and tango/ARNT gene fragments: testing monophyly of the subgenera *Ceratitis* (*Ceratitis*) and *C.* (*Pterandrus*). *Molecular Phylogenetics and Evolution*, 53: 412–424.

Blacket, M.J., Semeraro, L. & Malipatil, M.B. 2012. Barcoding Queensland fruit flies (*Bactrocera tryoni*): impediments and improvements. *Molecular Ecology Research*, 12: 428–436.

Bonizzoni, M., Guglielmino, C.R., Smallridge, C.J., Gomulski, M., Malacrida, A.R. & Gasperi, G. 2004. On the origins of medfly invasion and expansion in Australia. *Molecular Ecology*, 13: 3845–3855.

Bonizzoni, M., Malacrida, A.R., Guglielmino, C.R., Gomuslki, L.M., Gasperi, G. & Zheng, L. 2000. Microsatellite polymorphism in the Mediterranean fruit fly, *Ceratitis capitata*. *Insect Molecular Biology*, 9: 251–261.

Boykin, L.M., Schutze, M.K., Krosch, M.N., Chomic, A., Chapman, T.A., Englezou, A., Armstrong, K.F., Clarke, A.R., Hailstones, D. & Cameron, S.L. 2014. Multi-gene phylogenetic analysis of the south-east Asian pest members of the *Bactrocera dorsalis* species complex (Diptera: Tephritidae) does not support current taxonomy. *Journal of Applied Entomology*, 138: 235–253.

Buhay, J. 2009. "*COI*-like" sequences are becoming problematic in molecular systematic and DNA barcoding studies. *Journal of Crustacean Biology*, 29: 96–110.

Carroll, L.E., Norrbom, A.L., Dallwitz, M.J. & Thompson, F.C. 2004. *Pest fruit flies of the world: larvae*. Version: 9 April 2019. [Cited 24 January 2023] https://www.delta-intkey.com/ffl/ident.htm

Carroll, L.E. & Wharton, R.A. 1989. Morphology of the immature stages of *Anastrepha ludens* (Diptera: Tephritidae). *Annals of the Entomological Society of America*, 82: 201–214.

Catalá-Oltra, M., Llácer, E., Urbaneja, A. & Pérez-Hedo, M. 2020. Development and validation of real-time PCR method to estimate stored sperm in the spermathecae of *Ceratitis capitata* (Diptera: Tephritidae). *Journal of Economic Entomology*, 113: 1471–1478.

Copeland, R.S., Wharton, R.A., Quentin, L. & De Meyer, M. 2002. Indigenous hosts of *Ceratitis capitata* (Diptera: Tephritidae) in Kenya. *Annals of the Entomological Society of America*, 95: 672–694.

Davies, N., Villablanca, F.X. & Roderick, G.K. 1999. Bioinvasions of the medfly *Ceratitis capitata*: source estimation using DNA sequences at multiple intron loci. *Genetics*, 153: 351–360.

Delatte, H., Virgilio, M., Simiand, C., Quilici, S., Nzogella, Y.B. & Meyer, M. 2014. Isolation and characterisation of sixteen microsatellite markers amplifying an African agricultural pest, *Ceratitis rosa* (Walker) (Diptera: Tephritidae). *Conservation Genetics Resources*, 6: 9–11.

De Meyer, M. 1996. Revision of the subgenus *Ceratitis* (*Pardalaspis*) Bezzi, 1918 (Diptera: Tephritidae: Ceratitini). *Systematic Entomology*, 21: 15–26.

De Meyer, M. 1998. Revision of the subgenus *Ceratitis* (*Ceratalaspis*) Hancock (Diptera: Tephritidae). *Bulletin of Entomological Research*, 88: 257–290.

De Meyer, M. 1999. Phylogeny of the genus *Ceratitis* (Dacinae: Ceratitidini). In: M. Aluja & A.L. Norrbom, eds. *Fruit flies (Tephritidae) – Phylogeny and evolution of behavior*, pp. 409–428. Boca Raton, USA, CRC Press. 944 pp.

De Meyer, M. 2000. Systematic revision of the subgenus *Ceratitis* MacLeay *s.s.* (Diptera: Tephritidae). *Zoological Journal of the Linnean Society*, 128: 439–467.

De Meyer, M. 2001. Distribution patterns and host–plant relationships within the genus *Ceratitis* MacLeay (Diptera: Tephritidae) in Africa. *Cimbebasia*, 17: 219–228.

De Meyer, M. 2005. Phylogenetic relationships within the fruit fly genus *Ceratitis* MacLeay (Diptera: Tephritidae), derived from morphological and host plant evidence. *Insect Systematics and Evolution*, 36: 459–479.

De Meyer, M., Clarke, A.R., Vera T.M. & Hendrichs, J. 2015. Resolution of cryptic species complexes of tephritid pests to enhance SIT application and facilitate international trade – Editorial. *ZooKeys*, 540: 1–3.

De Meyer, M. & Copeland, R.S. 2001. Taxonomic notes on the Afrotropical subgenera *Ceratitis* (*Acropteromma*) Bezzi and *C.* (*Hoplolophomyia*) Bezzi (Diptera: Tephritidae). *Cimbebasia*, 17: 77–84.

De Meyer, M., Copeland, R.S., Lux, S.A., Mansell, M., Quilici, S., Wharton, R., White, I.M. & Zenz, N.J. 2002. *Annotated check list of host plants for Afrotropical fruit flies (Diptera: Tephritidae) of the genus* Ceratitis. Documentations Zoologiques, Musée Royal de l'Afrique Centrale, 27: 1–91.

De Meyer, M., Copeland, R.S., Wharton, R.A. & McPheron, B.A. 2004. On the geographic origin of the medfly, *Ceratitis capitata* (Wiedemann) (Diptera: Tephritidae). In: B.N. Barnes, ed. *Proceedings of the 6th International Symposium on Fruit Flies of Economic Importance*, 6–10 May 2002, Stellebosch, South Africa, pp. 45–53. Irene, South Africa, Isteg Scientific Publications.

De Meyer, M. & Freidberg, A. 2005. Revision of the subgenus *Ceratitis* (*Pterandrus*) Bezzi (Diptera: Tephritidae). *Israel Journal of Entomology*, 35–36: 197–315.

De Meyer, M., Mwatawala, M., Copeland, R.S. & Virgilio, M. 2016. Description of new *Ceratitis* species (Diptera: Tephritidae) from Africa, or how morphological and DNA data are complementary in discovering unknown species and matching sexes. *European Journal of Taxonomy*, 233: 1–23. http://dx.doi.org/10.5852/ejt.2016.233

DeSalle, R. & Goldstein, P. 2019. Review and interpretation on trends in DNA barcoding. *Frontiers in Ecology and Evolution*, 7: 302. https://doi.org/10.3389/fevo.2019.00302

Dhami, M.K., Gunawardana, D.N., Voice, D. & Kumarasinghe, L. 2016. A real-time PCR toolbox for accurate identification of invasive fruit fly species. *Journal of Applied Entomology*, 140: 536–552.

Douglas, L.J. & Haymer, D.S. 2001. Ribosomal ITS1 polymorphisms in *Ceratitis capitata* and *Ceratitis rosa* (Diptera: Tephritidae). *Annals of the Entomological Society of America*, 94: 726–731.

Duyck, P-F., David, P. & Quilici, S. 2006. Climatic niche partitioning following successive invasions by fruit flies in La Réunion. *Journal of Animal Ecology*, 75: 518–526.

EPPO (European and Mediterranean Plant Protection Organization). 2016. DNA barcoding as an identification tool for a number of regulated pests. PM 7/129 (1). *EPPO Bulletin*, 46: 501–537.

Epsky, N.D., Kendra, P.E. & Schnell, E.Q. 2014. History and development of food-based attractants. In: T.E. Shelly, N.D. Epsky, E.B. Jang, J. Reyes-Flores & R. Vargas, eds. *Trapping and the detection, control and regulation of tephritid fruit flies – Lures, area-wide programs, and trade implications*, pp. 75–118. Dordrecht, the Netherlands, Springer.

Erbout, N., Virgilio, M., Lens, L., Barr, N. & De Meyer, M. 2011. Discrepancies between subgeneric classification and molecular phylogeny of *Ceratitis* (Diptera: Tephritidae), can the evolution of host use provide some clues? *Molecular Phylogenetics and Evolution*, 60: 259–264.

Floyd, R., Lima, J., deWaard, J., Humble, L. & Hanner, R. 2010. Common goals: policy implications of DNA barcoding as a protocol for identification of arthropod pests. *Biological Invasions*, 12: 2947–2954.

Folmer, O., Black, M., Hoeh, W., Lutz, R. & Vrijenhoek, R. 1994. DNA primers for amplification of mitochondrial cytochrome c oxidase subunit I from diverse metazoan invertebrates. *Molecular Marine Biology and Biotechnology*, 3: 294–299.

Foote, R.H., Blanc, F.L. & Norrbom, A.L. 1993. *Handbook of the fruit flies (Diptera: Tephritidae) of America north of Mexico*. Ithaca, USA, Comstock Publishing Associates (Cornell University Press). 571 pp.

Frey, J.E., Guillíen, L., Frey, B., Samietz, J., Rull, J. & Aluja, M. 2013. Developing diagnostic SNP panels for the identification of true fruit flies (Diptera: Tephritidae) within the limits of *COI*-based species delimitation. *BMC Evolutionary Biology*, 13: 106. http://www.biomedcentral.com/1471-2148/13/106

Frías Lasserre, D., Hernández Ortiz, V. & López Muñoz, L. 2009. Description of the third-instar of *Anastrepha leptozona* Hendel (Diptera: Tephritidae). *Neotropical Entomology*, 38(4): 491–496.

Frías, D., Hernández-Ortiz, V., Vaccaro, N.C., Bartolucci, A.F. & Salles, L.A. 2006. Comparative morphology of immature stages in some frugivorous species of fruit flies (Diptera: Tephritidae). In: A. Freidberg, ed. Biotaxonomy of the Tephritoidea, *Israel Journal of Entomology*, 35–36: 423–457.

Frías, D., Selivon, D. & Hernández-Ortiz, V. 2008. Taxonomy of immature stages: new morphological characters for Tephritidae larvae identification. In: A. Malavasi, R. Sugayama, R. Zucchi & J. Sivinski, eds. *Fruit flies of economic importance – From basic to applied knowledge*. Proceedings of the 7th International Symposium on Fruit Flies of Economic Importance, Salvador, Brazil, 10–15 September 2006, pp. 29–44.

Gasparich, G.E., Silva, J.G., H-Y. Han, H-Y., McPheron, B.A., Steck, G.J. & Sheppard, W.S. 1997. Population genetic structure of Mediterranean fruit fly (Diptera: Tephritidae) and implications for worldwide colonization patterns. *Annals of the Entomological Society of America*, 90: 790–797.

Hancock, D.L. 1984. Ceratitinae (Diptera: Tephritidae) from the Malagasy subregion. *Journal of the Entomological Society of Southern Africa*, 47: 277–301.

Hebert, P.D.N., Cywinska, A., Ball, S.L. & deWaard, J.R. 2003. Biological identifications through DNA barcodes. *Proceedings of the Royal Society B*, 270: 313–321.

Huang, C.-G., Hsu, J.-C., Haymer, D.S., Lin, G.-C. & Wu, W.-J. 2009. Rapid identification of the Mediterranean fruit fly (Diptera: Tephritidae) by loop-mediated isothermal amplification. *Journal of Economic Entomology*, 102: 1239–1246.

Jiang, F., Jin, Q., Liang, L., Zhang, A.B. & Li, Z.H. 2014. Existence of species complex largely reduced barcoding success for invasive species of Tephritidae: a case study in *Bactrocera* spp. *Molecular Ecology Resources*, 14: 1114–1128.

Juan-Blasco, M., Urbaneja, A., San Andrés, V., Castañera, P. & Sabater-Muñoz, B. 2013. Improving the sterile sperm identification method for its implementation in the area-wide sterile insect technique program against *Ceratitis capitata* (Diptera: Tephritidae) in Spain. *Journal of Economic Entomology*, 106: 2541–2547.

Kandybina, M.N. 1977. Lichinki plodovykh mukh-pestrokrylok (Diptera, Tephritidae). [Larvae of fruit-infesting fruit flies (Diptera, Tephritidae).] *Opred. Faune SSSR*, 114: 1–210 (in Russian; unpublished English translation, 1987, produced by National Agricultural Library, Beltsville, Maryland, USA).

Liquido, N., McQuate, G. & Suiter, K. 2016. USDA compendium of fruit fly host information (CoFFHI). In: B. Sabater-Muñoz, T. Vera, R. Pereira & W. Orankanok, eds. *Proceedings of the 9th International Symposium on Fruit Flies of Economic Importance*, 12–16 May 2014, Bangkok, Thailand, pp. 420–434.

Manrakhan, A., Daneel, J.-H., Beck, R., Virgilio, M., Meganck, K. & De Meyer, M. 2017. Efficacy of trapping systems for monitoring of Afrotropical fruit flies. *Journal of Applied Entomology*, 141: 825–840.

Meier, R., Shiyang, K., Vaidya, G. & Ng, P.K.L. 2006. DNA barcoding and taxonomy in Diptera: a tale of high intraspecific variability and low identification success. *Systematic Biology*, 55(5): 715–728.

Meixner, M.D., McPheron, B.A., Silva, J.G., Gasparich, G.E. & Sheppard, W.S. 2002. The Mediterranean fruit fly in California: evidence for multiple introductions and persistent

populations based on microsatellite and mitochondrial DNA variability. *Molecular Ecology*, 11: 891–899.

Mwatawala, M.W., Virgilio, M., Quilici, S., Dominic, M. & De Meyer, M. 2013. Field evaluation of the relative attractiveness of enriched ginger root oil (EGO) lure and trimedlure for African *Ceratitis* species (Diptera: Tephritidae). *Journal of Applied Entomology*, 137: 392–397.

Plant Health Australia. 2016. *The Australian handbook for the identification of fruit flies*, version 2.1. Canberra. 314 pp.

Rodriguez, E.J., Steck, G.J., Moore, M.R., Norrbom, A.L., Sutton, B.D. & Branham, M.A. 2021. Description of larvae of *Anastrepha amplidentata* and *Anastrepha durantae* with review of larval morphology of the *fraterculus* group (Diptera: Tephritidae). *Proceedings of the Entomological Society of Washington*, 123(1): 169–189.

Ruiz-Arce, R., Todd, T.N., Deleon, R., Barr, N.B., Virgilio, M., De Meyer, M. & McPheron, B.A. 2020. Worldwide phylogeography of *Ceratitis capitata* (Diptera: Tephritidae) using mitochondrial DNA. *Journal of Economic Entomology*, 113: 1455–1470.

San Andrés, V., Urbaneja, A., Sabater-Muñoz, B. & Castañera, P. 2007. A novel molecular approach to assess mating success of sterile *Ceratitis capitata* (Diptera: Tephritidae) males in sterile insect technique programs. *Journal of Economic Entomology*, 100: 1444–1449.

Sim, S.B., Ruiz-Arce, R., Barr, N.B. & Geib, S.M. 2017. A new diagnostic resource for *Ceratitis capitata* strain identification based on QTL mapping. *G3: Genes|Genomes|Genetics*, 7: 3637–3647.

Simon, C., Frati, F., Beckenbach, A., Crespi, B., Liu, H. & Flook, P. 1994. Evolution, weighting, and phylogenetic utility of mitochondrial gene sequences and a compilation of conserved polymerase chain reaction primers. *Annals of the Entomological Society of America*, 87: 651–701.

Steck, G.J. & Ekesi, S. 2015. Description of third-instar larvae of *Ceratitis fasciventris*, *C. anonae*, *C. rosa* (FAR complex) and *C. capitata* (Diptera, Tephritidae). *ZooKeys*, 540: 443–466.

Steck, G.J., Ndlela, S., Somma, L.A., Diaz, J., Moore, M.J. & Awad, J. (2022). Description of the immature stages of *Dacus bivittatus* (Diptera: Tephritidae), the greater pumpkin fruit fly. *Proceedings of the Entomological Society of Washington*, 124: 661–682.

Steck, G.J. & Wharton, R.A. 1988. Description of immature stages of *Anastrepha interrupta*, *A. limae*, and *A. grandis* (Diptera: Tephritidae). *Annals of the Entomological Society of America*, 81: 994–1003.

Tan, K.H., Nishida, R., Jang, E.B. & Shelly, T.E. 2014. Pheromones, male lures, and trapping of tephritid fruit flies. In: T. Shelly, N. Epsky, E.B. Jang, J. Reyes-Flores & R. Vargas, eds. *Trapping and the detection, control, and regulation of tephritid fruit flies – Lures, area-wide programs and trade implications*, pp. 15–74. Dordrecht, the Netherlands, Springer.

Teskey, H.J. 1981. Morphology and terminology: larvae. In: J.F. McAlpine, B.V. Peterson, G.E. Shewell, H.J. Teskey, J.R. Vockeroth & D.M. Wood, coords. *Manual of Nearctic Diptera, Volume 1*. Research Branch Agriculture Canada, Monograph 27: 65–88.

USDA (United Stated Department of Agriculture). 2023. *USDA compendium of fruit fly host information*, Edition 5.0. USA, USDA Animal and Plant Health Inspection Service & Agricultural Research Service. [Cited 27 January 2023]. https://coffhi.cphst.org

Virgilio, M., Backeljau, T., Barr, N. & De Meyer, M. 2008. Molecular evaluation of nominal species in the *Ceratitis fasciventris*, *C. anonae*, *C. rosa* complex (Diptera: Tephritidae). *Molecular Phylogenetics and Evolution*, 48: 270–280.

Virgilio, M., Backeljau, T., Nevado, B. & De Meyer, M. 2010. Comparative performances of DNA barcoding across insect orders. *BMC Bioinformatics*, 11: 206. https://doi.org/10.1186/1471-2105-11-206

Virgilio, M., Daneel, J.-H., Manrakhan, A., Delatte, H., Meganck, K. & De Meyer, M. 2019. An integrated diagnostic setup for the morphological and molecular identification of the *Ceratitis*

FAR complex (*C. anonae*, *C. fasciventris*, *C. rosa*, *C. quilicii*, Diptera, Tephritidae). *Bulletin of Entomological Research*, 109: 376–382.

Virgilio, M., Delatte, H., Nzogela, Y.B., Simiand, C., Quilici, S., De Meyer, M. & Mwatawala, M. 2015. Population structure and cryptic genetic variation in the mango fruit fly, *Ceratitis cosyra* (Diptera, Tephritidae). *ZooKeys*, 540: 525–538.

Virgilio, M., Delatte, H., Quilici, S., Backeljau, T. & De Meyer, M. 2013. Cryptic diversity and gene flow among three African agricultural pests: *Ceratitis rosa*, *Ceratitis fasciventris* and *Ceratitis anonae* (Diptera, Tephritidae). *Molecular Ecology*, 22: 2526–2539.

Virgilio, M., Jordaens, K., Breman, F.C., Backeljau, T. & De Meyer, M. 2012. Identifying insects with incomplete DNA barcode libraries, African fruit flies (Diptera: Tephritidae) as a test case. *PLoS ONE*, 7: e31581. https://doi.org/10.1371/journal.pone.0031581

Virgilio, M., Manrakhan, A., Delatte, H., Daneel, J-H., Mwatawala, M.W., Meganck, K., Barr, N.B. & De Meyer, M. 2017. The complex case of *Ceratitis cosyra* (Diptera, Tephritidae) and relatives. A DNA barcoding perspective. *Journal of Applied Entomology*, 141: 788–797.

Virgilio, M., White, I. & De Meyer, M. 2014. A set of multi-entry identification keys to African frugivorous flies (Diptera, Tephritidae). *ZooKeys*, 428: 97–108.

White, I.M. & Elson-Harris, M.M. 1992. *Fruit flies of economic significance: their identification and bionomics*. Wallingford, UK, CABI. 601 pp.

White, I.M., Headrick, D.H., Norrbom, A.L. & Carroll, L.E. 1999. Glossary. In: M. Aluja & A.L. Norrbom, eds. *Fruit flies (Tephritidae) – Phylogeny and evolution of behavior*, pp. 881–924. Boca Raton, USA, CRC Press. 944 pp.

Zhang Y., Meyer M.D., Virgilio M, Feng S.Q, Badji K, & Li Z.H. 2021. Phylogenomic resolution of the *Ceratitis* FARQ complex (Diptera: Tephritidae). *Molecular Phylogenetics and Evolution*, 161: 107160.

9. Figures

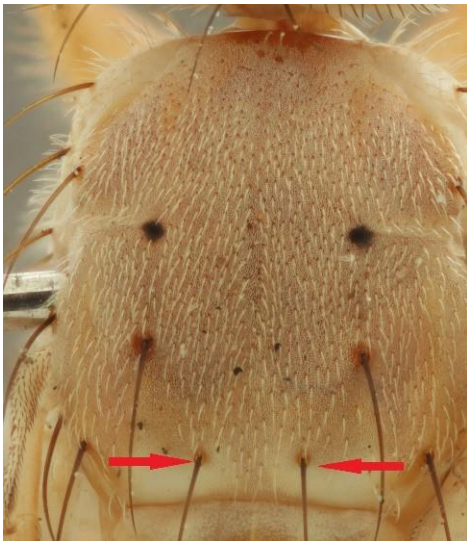

Figure 1. Scutum of *Ceratitis quinaria*: acrostichal setae present (indicated by arrows).

Source: Jonathan Brecko and Annelies Kayenbergh, © Royal Museum for Central Africa, Belgium.

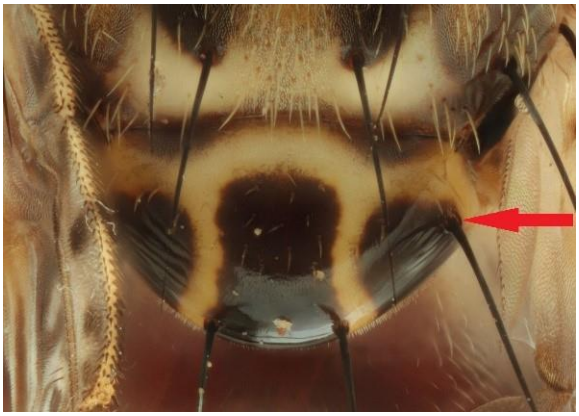

Figure 2. Scutellum of *Ceratitis rosa*: basal scutellar setae present (indicated by arrow); swollen, apically with three separated markings.

Source: Jonathan Brecko and Annelies Kayenbergh, © Royal Museum for Central Africa, Belgium.

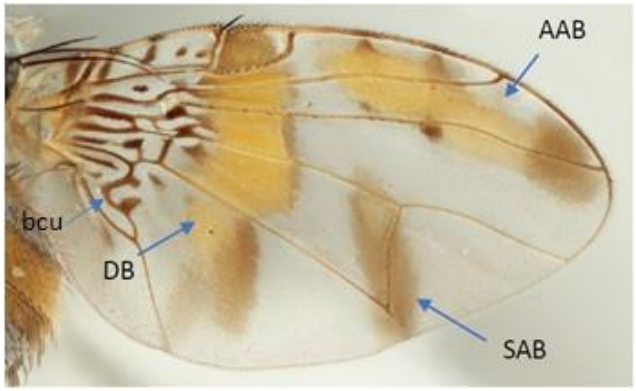

Figure 3. Wing of *Ceratitis capitata*.

Notes: AAB, anterior apical band; bcu, wing cell bcu (indicating location of constriction at base); DB, discal band; SAB, subapical band.

Source: Jonathan Brecko and Annelies Kayenbergh, © Royal Museum for Central Africa, Belgium.

Figure 4. Scutellum of *Perilampsis tetradactyla*: flat.

Source: Jonathan Brecko and Annelies Kayenbergh, © Royal Museum for Central Africa, Belgium.

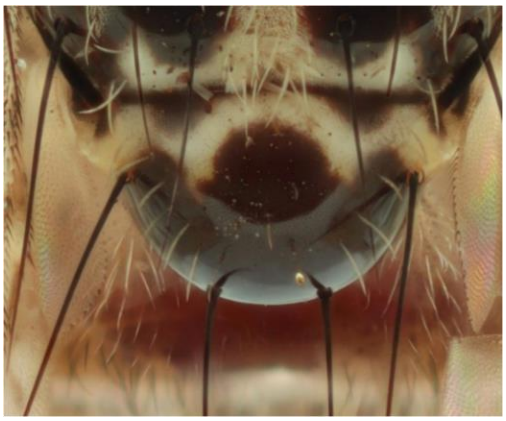

Figure 5. Scutellum of *Ceratitis capitata*: apical markings fused.

Source: Jonathan Brecko and Annelies Kayenbergh, © Royal Museum for Central Africa, Belgium.

Figure 6. Scutellum of *Ceratitis gravinotata*: apical markings covering most of scutellar dorsal surface.

Source: Jonathan Brecko and Annelies Kayenbergh, © Royal Museum for Central Africa, Belgium.

Figure 7. Scutellum of *Ceratitis quinaria*: apical markings reduced to small dark spots.

Source: Jonathan Brecko and Annelies Kayenbergh, © Royal Museum for Central Africa, Belgium.

Figure 8. Scutellum of *Capparimyia savastani*: two dark markings.

Source: Jonathan Brecko and Annelies Kayenbergh, © Royal Museum for Central Africa, Belgium.

Figure 9. Scutellum of *Trirhithrum obscurum*: largely to completely black dorsal surface.

Source: Jonathan Brecko and Annelies Kayenbergh, © Royal Museum for Central Africa, Belgium.

Figure 10. Scutellum of *Neoceratitis cyanescens*: apically with single dark marking.

Source: Jonathan Brecko and Annelies Kayenbergh, © Royal Museum for Central Africa, Belgium.

Figure 11. Wing of *Ceratitis rubivora*: posterior apical band (indicated by arrow) present.

Source: Jonathan Brecko and Annelies Kayenbergh, © Royal Museum for Central Africa, Belgium.

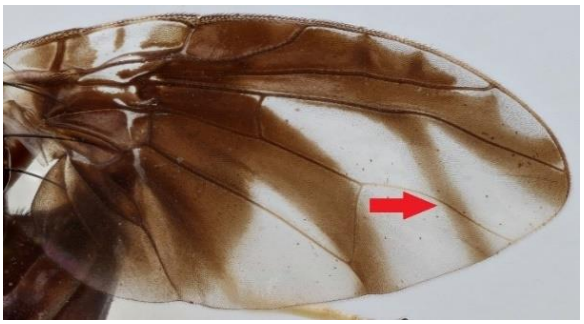

Figure 12. Wing of *Trirhithrum nitidum*: wing posterior apical band (indicated by arrow) present.

Source: Jonathan Brecko and Annelies Kayenbergh, © Royal Museum for Central Africa, Belgium.

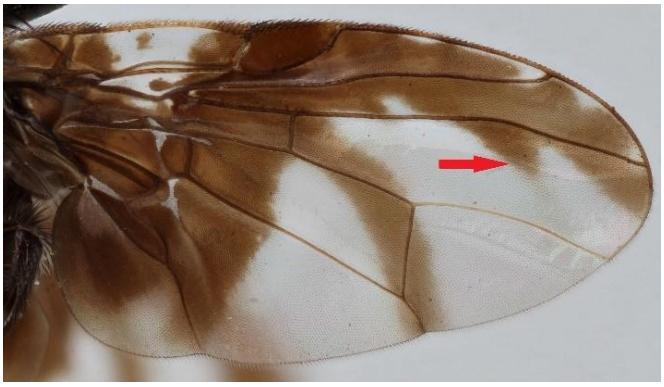

Figure 13. Wing of *Trirhithrum occipitale*: wing posterior apical band reduced to toothlike appendage (indicated by arrow).

Source: Jonathan Brecko and Annelies Kayenbergh, © Royal Museum for Central Africa, Belgium.

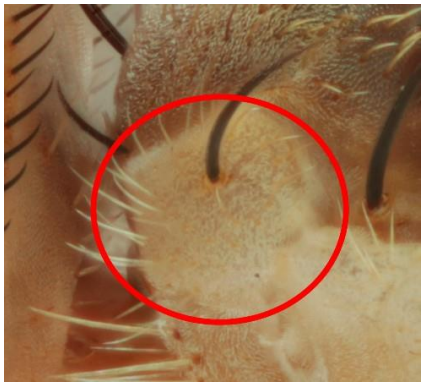

Figure 14. Postpronotal lobe (lateral view, indicated by circle) of *Ceratitis rosa*: unicolorous.

Source: Jonathan Brecko and Annelies Kayenbergh, © Royal Museum for Central Africa, Belgium.

Figure 15. Postpronotal lobe (dorsal view, indicated by circle) of *Ceratitis quinaria*: unicolorous.

Source: Jonathan Brecko and Annelies Kayenbergh, © Royal Museum for Central Africa, Belgium.

Figure 16. Postpronotal lobe (lateral view, indicated by circle) of *Ceratitis capitata*: pale with black median spot.

Source: Jonathan Brecko and Annelies Kayenbergh, © Royal Museum for Central Africa, Belgium.

Figure 17. Postpronotal lobe (dorsal view, indicated by circle) of *Ceratitis caetrata*: pale with black median spot.

Source: Jonathan Brecko and Annelies Kayenbergh, © Royal Museum for Central Africa, Belgium.

Figure 18. Scutellum of *Ceratitis rosa*: apically with three separate dark spots.

Source: Jonathan Brecko and Annelies Kayenbergh, © Royal Museum for Central Africa, Belgium.

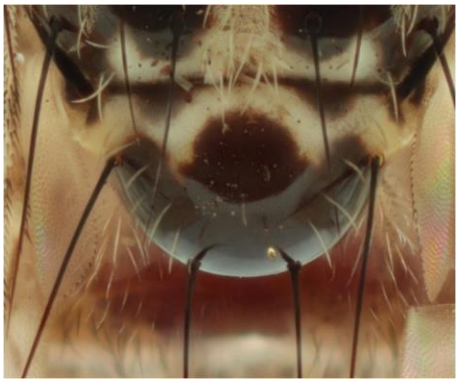

Figure 19. Scutellum of *Ceratitis capitata*: apical spots merged into one marking.

Source: Jonathan Brecko and Annelies Kayenbergh, © Royal Museum for Central Africa, Belgium.

Figure 20. Scutum of *Ceratitis rosa*: greyish to greyish-brown with indistinct darker markings.

Source: Jonathan Brecko and Annelies Kayenbergh, © Royal Museum for Central Africa, Belgium.

Figure 21. Scutum of *Ceratitis capitata*: grey with distinct black markings.

Source: Jonathan Brecko and Annelies Kayenbergh, © Royal Museum for Central Africa, Belgium.

Figure 22. Scutum of *Ceratitis cosyra*: yellow-orange to orange ground colour with distinct black markings.

Source: Jonathan Brecko and Annelies Kayenbergh, © Royal Museum for Central Africa, Belgium.

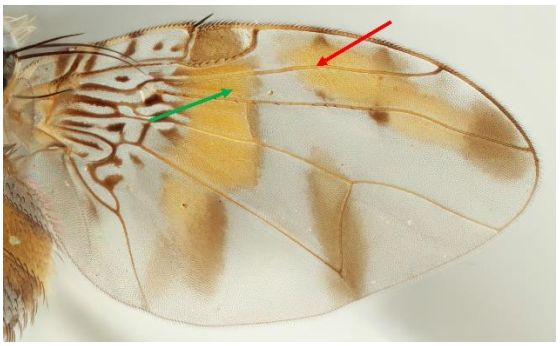

Figure 23. Wing of *Ceratitis capitata*: anterior apical band (indicated by red arrow) completely separated from discal band (indicated by green arrow).

Source: Jonathan Brecko and Annelies Kayenbergh, © Royal Museum for Central Africa, Belgium.

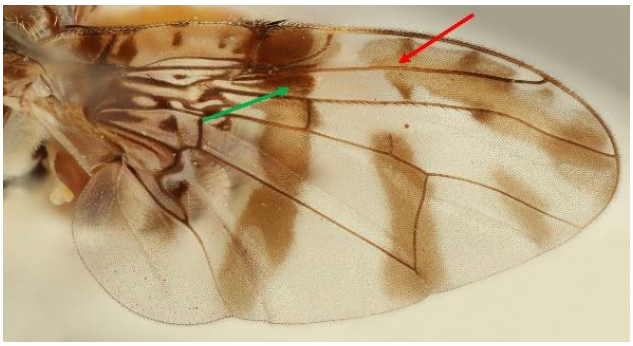

Figure 24. Wing of *Ceratitis rubivora*: anterior apical band (indicated by red arrow) completely separated from discal band (indicated by green arrow).

Source: Jonathan Brecko and Annelies Kayenbergh, © Royal Museum for Central Africa, Belgium.

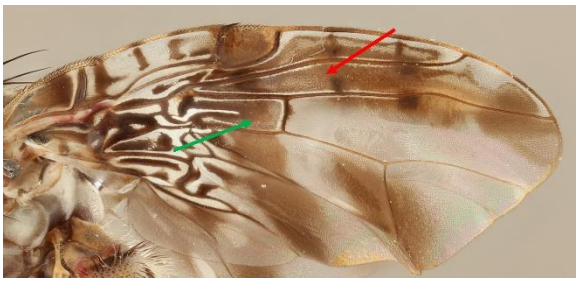

Figure 25. Wing of *Ceratitis edwardsi*: anterior apical band (indicated by red arrow) connected with discal band (indicated by green arrow).

Source: Jonathan Brecko and Annelies Kayenbergh, © Royal Museum for Central Africa, Belgium.

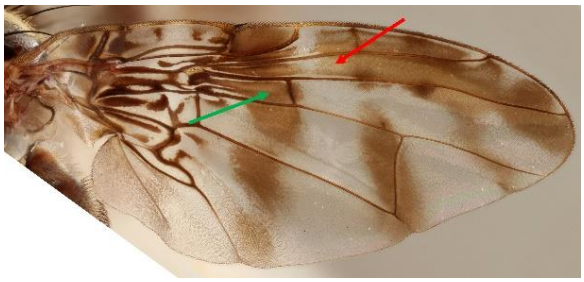

Figure 26. Wing of *Ceratitis cuthbertsoni*: anterior apical band (indicated by red arrow) partially separated from discal band (indicated by green arrow).

Source: Jonathan Brecko and Annelies Kayenbergh, © Royal Museum for Central Africa, Belgium.

Figure 27. Abdomen of *Ceratitis colae*: third tergum with black-brown transverse band.

Source: Jonathan Brecko and Annelies Kayenbergh, © Royal Museum for Central Africa, Belgium.

Figure 28. Abdomen of *Ceratitis argenteobrunnea*: third tergum without black-brown transverse band.

Source: Jonathan Brecko and Annelies Kayenbergh, © Royal Museum for Central Africa, Belgium.

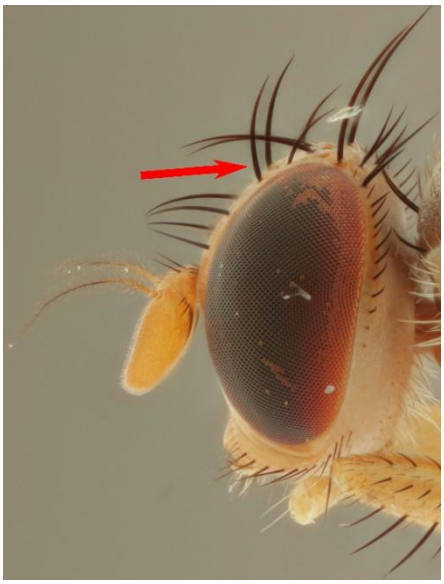

Figure 29. Male head of *Ceratitis rosa* (lateral view): lower orbital seta bristle-like, not modified apically (indicated by arrow).

Source: Jonathan Brecko and Annelies Kayenbergh, © Royal Museum for Central Africa, Belgium.

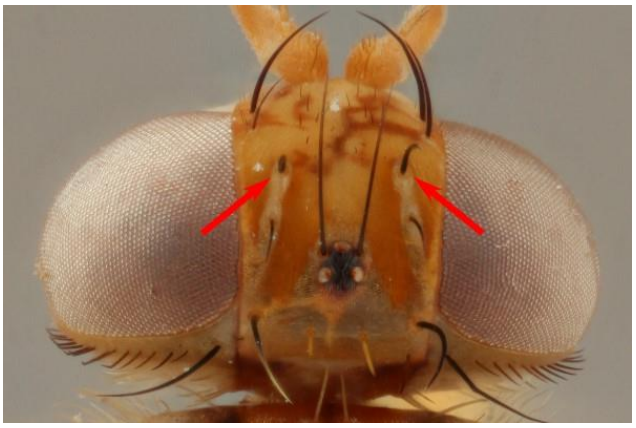

Figure 30. Male head of *Ceratitis cosyra* (dorsal view): lower orbital seta bristle-like, not modified apically (indicated by arrow).

Source: Jonathan Brecko and Annelies Kayenbergh, © Royal Museum for Central Africa, Belgium.

Figure 31. Male head of *Ceratitis capitata* (lateral view): lower orbital seta modified, flattened at apex (indicated by arrow).

Source: Jonathan Brecko and Annelies Kayenbergh, © Royal Museum for Central Africa, Belgium.

Figure 32. Male head of *Ceratitis capitata* (dorsal view): lower orbital seta modified, flattened at apex (indicated by arrow).

Source: Jonathan Brecko and Annelies Kayenbergh, © Royal Museum for Central Africa, Belgium.

Figure 33. Leg fore femur of *Ceratitis anonae*: posteriorly with dispersed setae and with few dark hairs between posterior and posterodorsal row of setae.

Source: Jonathan Brecko and Annelies Kayenbergh, © Royal Museum for Central Africa, Belgium.

Figure 34. Leg fore femur of *Ceratitis quinaria*: posteriorly with dispersed setae but without dark hairs between posterior and posterodorsal setae.

Source: Jonathan Brecko and Annelies Kayenbergh, © Royal Museum for Central Africa, Belgium.

Figure 35. Leg fore femur of *Ceratitis malgassa*: posteriorly with bush of dense setae.

Source: Jonathan Brecko and Annelies Kayenbergh, © Royal Museum for Central Africa, Belgium.

Figure 36. Male leg, mid femur of *Ceratitis anonae*: ventrally with row of long stout setae ("feathering").

Source: Jonathan Brecko and Annelies Kayenbergh, © Royal Museum for Central Africa, Belgium.

Figure 37. Male leg, mid femur of *Ceratitis quilicii*: ventrally with few dispersed long but thin setae.

Source: Jonathan Brecko and Annelies Kayenbergh, © Royal Museum for Central Africa, Belgium.

Figure 38. Male leg, mid tibia of *Ceratitis rubivora*: row of long black stout setae (feathering) along lateral margins for more than three-quarters of entire length, and pale to brownish over entire length.

Source: Jonathan Brecko and Annelies Kayenbergh, © Royal Museum for Central Africa, Belgium.

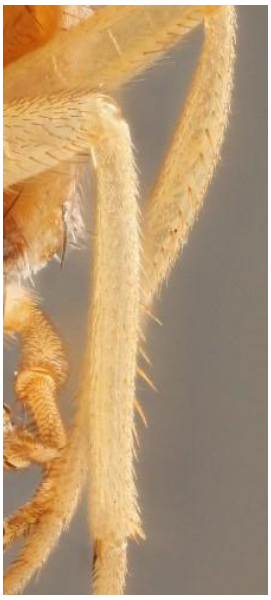

Figure 39. Male leg, mid tibia of *Ceratitis argenteobrunnea*: dorsal and ventral sides with few dispersed short setae and pale coloured over entire length.

Source: Jonathan Brecko and Annelies Kayenbergh, © Royal Museum for Central Africa, Belgium.

Figure 40. Male leg, mid tibia of *Ceratitis fasciventris*: row of long stout setae (feathering) along lateral margins for less than half of apical part and usually pale coloured, at most area between feathering partially darker yellow to brownish coloured.

Source: Jonathan Brecko and Annelies Kayenbergh, © Royal Museum for Central Africa, Belgium.

Figure 41. Male leg, mid tibia of *Ceratitis quilicii*: row of long stout setae (feathering) along lateral margins for more than half but less than three-quarters of entire length and pale except area between feathering where darker coloured; dark colour not reaching lateral margins in upper part (indicated by arrow).

Source: Jonathan Brecko and Annelies Kayenbergh, © Royal Museum for Central Africa, Belgium.

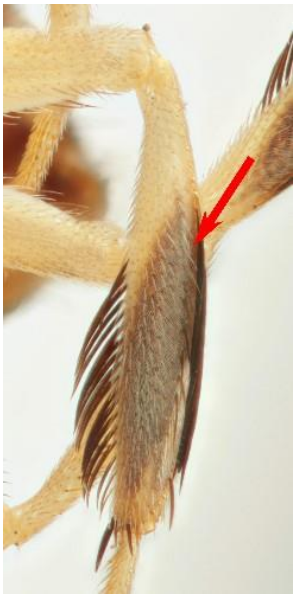

Figure 42. Male leg, mid tibia of *Ceratitis rosa*: row of long stout setae (feathering) along lateral margins for more than half but less than three-quarters of entire length and pale except area between feathering where darker coloured; dark colour reaching lateral margins in upper part (indicated by arrow).

Source: Jonathan Brecko and Annelies Kayenbergh, © Royal Museum for Central Africa, Belgium.

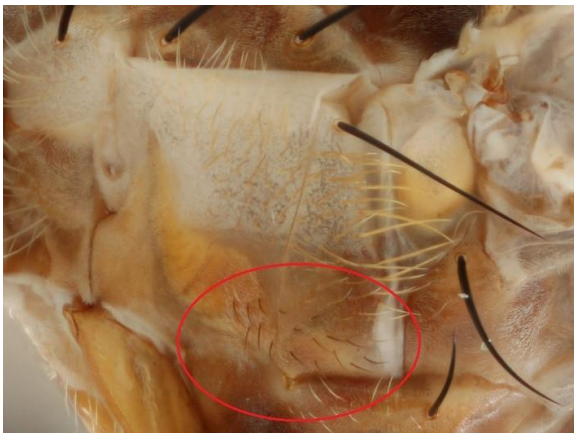

Figure 43. Female anepisternum of *Ceratitis anonae*: ventral margin with partly dark setulae (few dark hairs) along it (indicated by circle).

Source: Jonathan Brecko and Annelies Kayenbergh, © Royal Museum for Central Africa, Belgium.

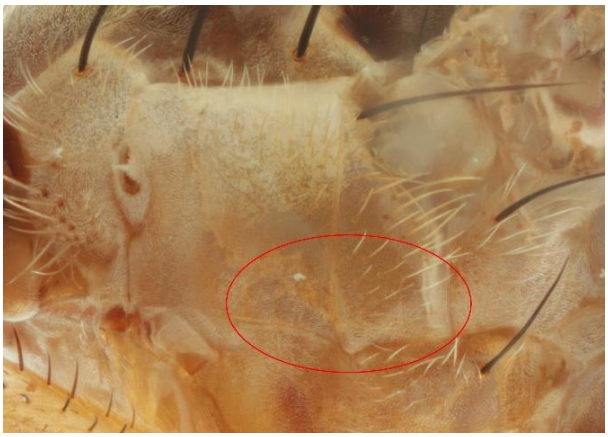

Figure 44. Female anepisternum of *Ceratitis rosa*: ventral margin without dark hairs along it, pilosity entirely pale (indicated by circle).

Source: Jonathan Brecko and Annelies Kayenbergh, © Royal Museum for Central Africa, Belgium.

Figure 45. From top to bottom: egg, first instar, second instar and third instar of *Ceratitis capita*, showing differences in sizes.

Source: Gary J. Steck, Florida Department of Agriculture and Consumer Services, United States of America.

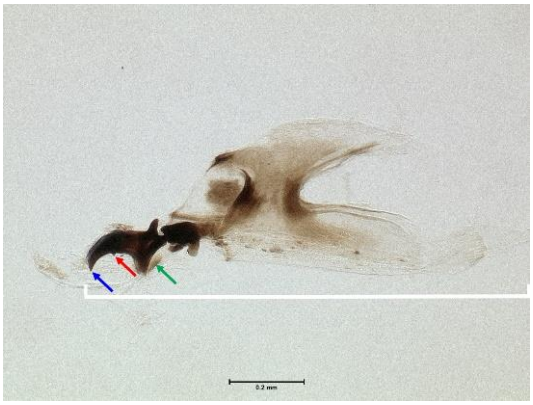

Figure 46. Cephaloskeleton of *Ceratitis fasciventris*, third instar: subapical tooth (red arrow) on mouthhook is much smaller than apical tooth (blue arrow); dental sclerite present (green arrow).

Notes: White bar = length of cephaloskeleton. Black scale bar = 0.2 mm.

Source: Gary J. Steck, Florida Department of Agriculture and Consumer Services, United States of America.

Figure 47. Cephaloskeleton of *Ceratitis fasciventris*, second instar: subapical tooth on mouthhook is subequal in size to apical tooth.

Source: Gary J. Steck, Florida Department of Agriculture and Consumer Services, United States of America.

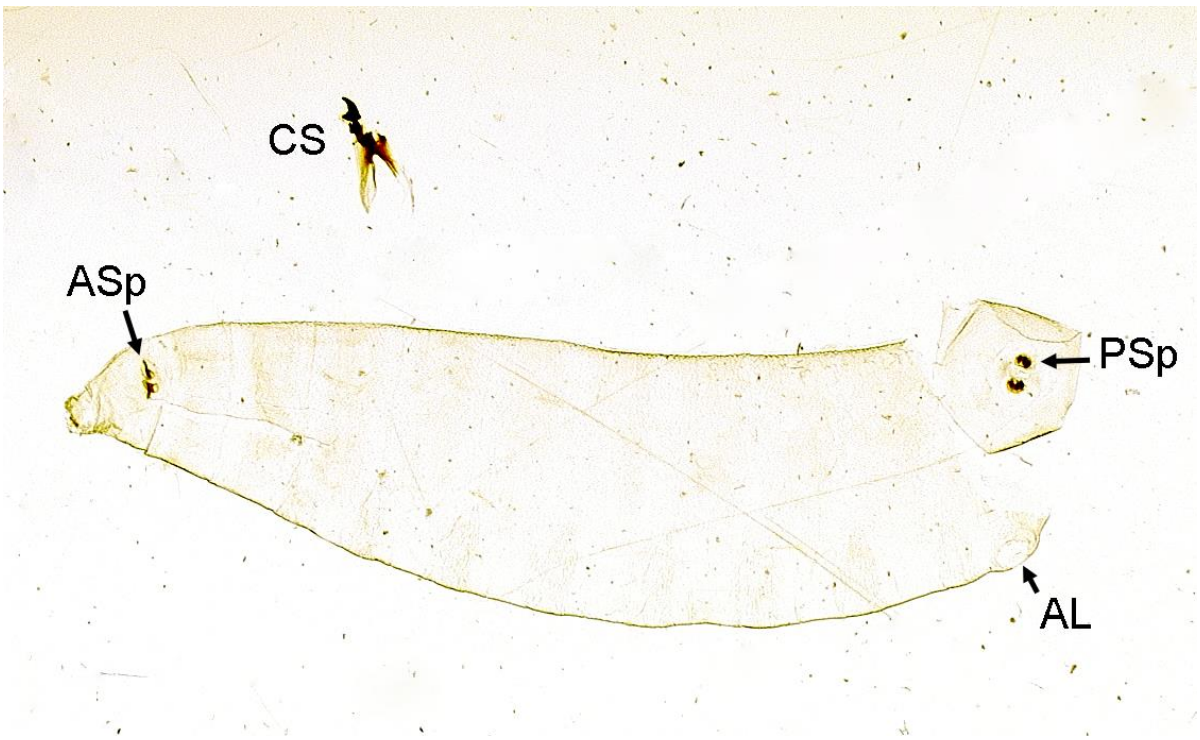

Figure 48. Slide-mounted, cleared cuticle with cephaloskeleton removed.

Notes: AL, anal lobe; ASp, anterior spiracle; CS, cephaloskeleton; PSp, posterior spiracle.

Source: Gary J. Steck, Florida Department of Agriculture and Consumer Services, United States of America.

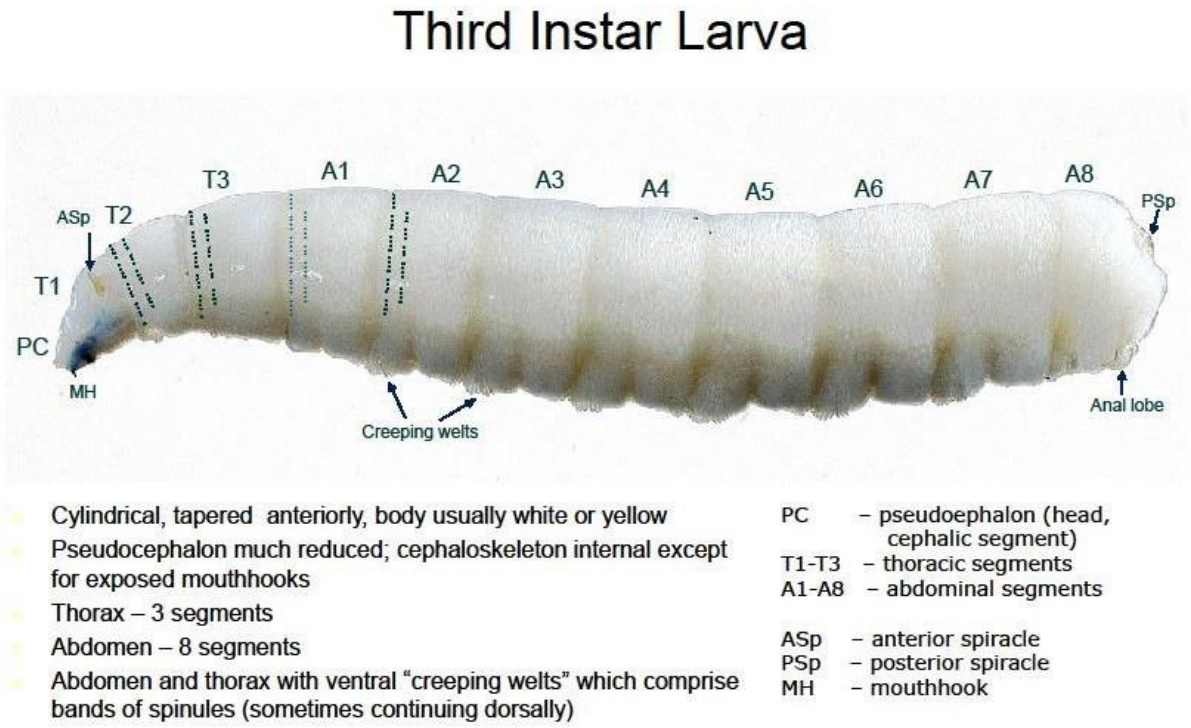

Figure 49. Habitus of fruit fly larva showing location of major anatomical features.

Source: Gary J. Steck, Florida Department of Agriculture and Consumer Services, United States of America.

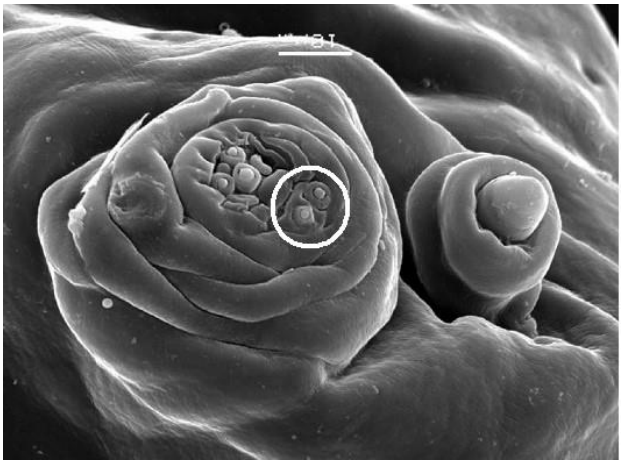

Figure 50. Maxillary palpus, dorsolateral pair of sensilla (circle) and antenna of *Ceratitis capitata* (scanning electron micrograph).

Source: Louis A. Somma, Florida Department of Agriculture and Consumer Services, United States of America.

Figure 51. Maxillary palpus, dorsolateral pair of sensilla (circle) and antenna of *Ceratitis capitata* (light photomicrograph).

Source: Jessica Diaz, Florida Department of Agriculture and Consumer Services, United States of America.

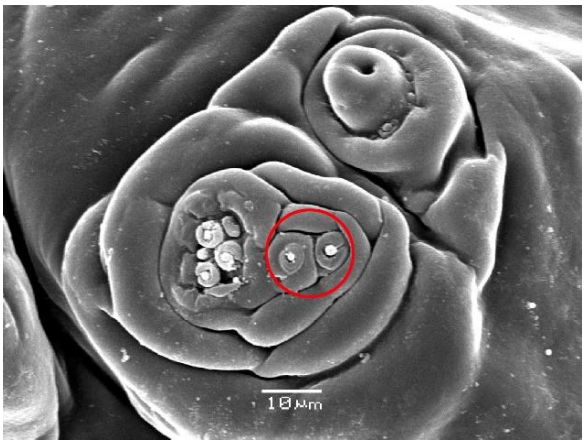

Figure 52. Maxillary palpus, dorsolateral pair of sensilla (circle) and antenna of *Anastrepha ludens* (scanning electron micrograph).

Source: Louis A. Somma, Florida Department of Agriculture and Consumer Services, United States of America.

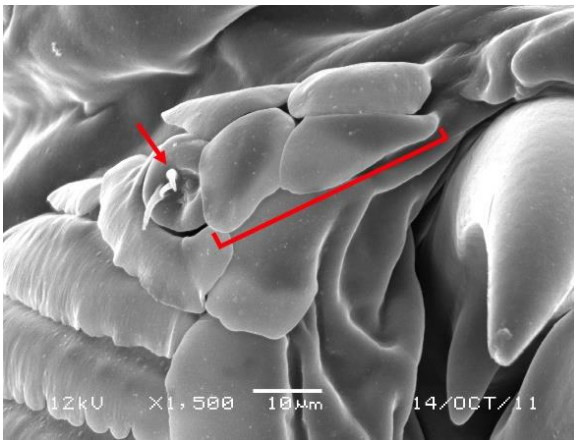

Figure 53. Preoral organ (arrow) and preoral lobes (red bar) of *Ceratitis cosyra*.

Source: Gary J. Steck, Florida Department of Agriculture and Consumer Services, United States of America.

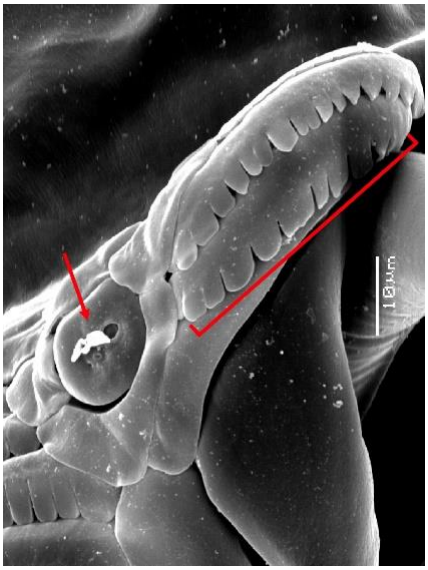

Figure 54. Preoral organ (arrow) and preoral lobes (red bar) of *Zeugodacus cucurbitae*.

Source: Louis A. Somma, Florida Department of Agriculture and Consumer Services, United States of America.

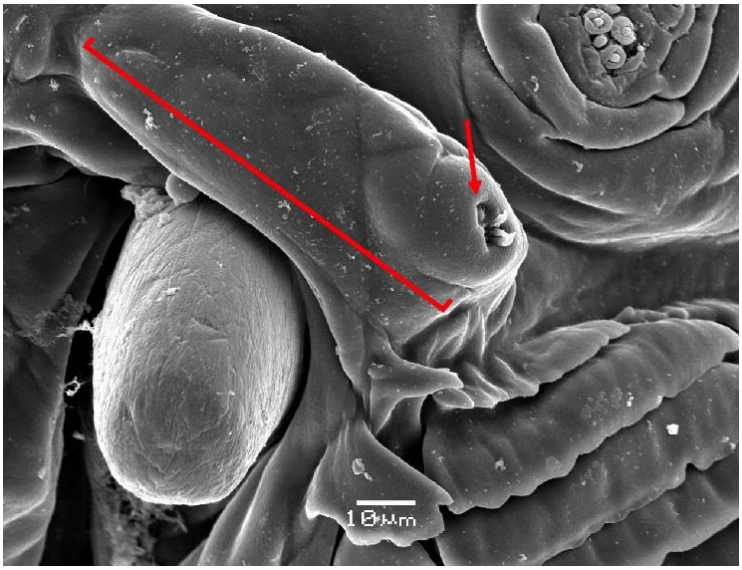

Figure 55. Preoral organ (arrow) and preoral lobes (red bar) of *Anastrepha ludens*.

Source: Louis A. Somma, Florida Department of Agriculture and Consumer Services, United States of America.

Figure 56. Preoral teeth (circle) of *Rhagoletis pomonella*.

Source: Gary J. Steck, Florida Department of Agriculture and Consumer Services, United States of America.

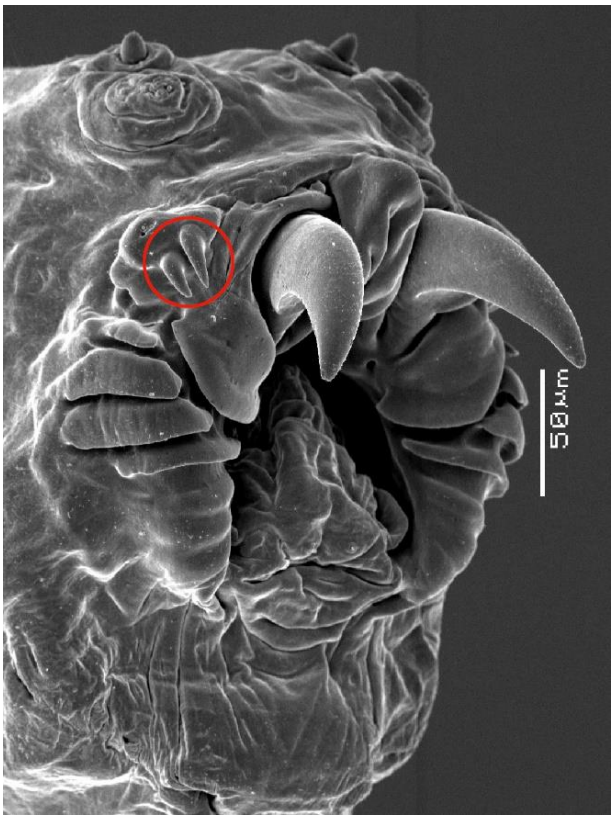

Figure 57. Preoral teeth (circle) of *Rhagoletis pomonella* (scanning electron micrograph).

Source: Louis A. Somma, Florida Department of Agriculture and Consumer Services, United States of America.

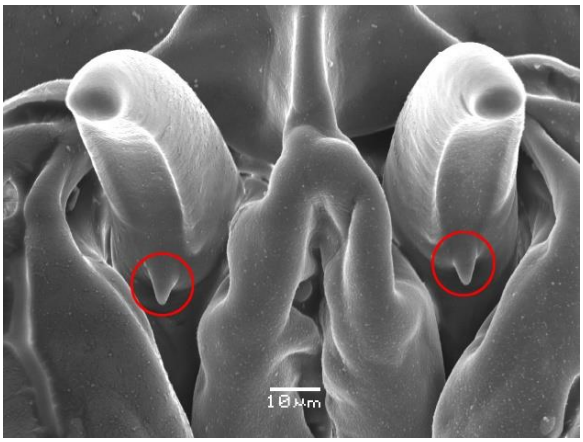

Figure 58. Mouthhooks of *Ceratitis rosa*: with grooved ventral surface and small subapical teeth (circles).

Source: Gary J. Steck, Florida Department of Agriculture and Consumer Services, United States of America.

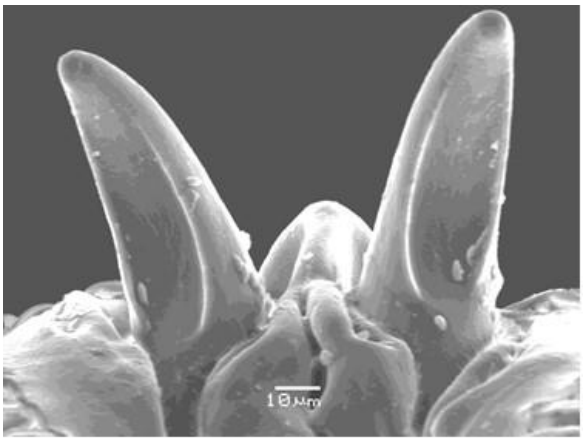

Figure 59. Mouthhooks of *Ceratitis capitata*: with grooved ventral surface and no teeth.

Source: Gary J. Steck, Florida Department of Agriculture and Consumer Services, United States of America.

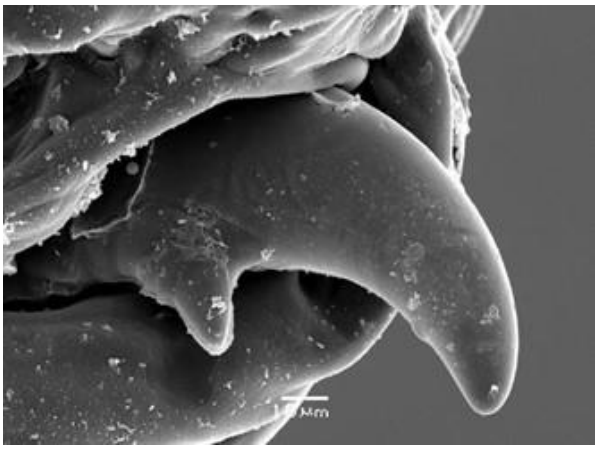

Figure 60. Mouthhook of *Dacus bivittatus*: tusk-shaped with large subapical tooth.

Source: Louis A. Somma, Florida Department of Agriculture and Consumer Services, United States of America.

Figure 61. Mouthhook of *Ceratitis capitata*: with elongate posterior neck (arrows).

Source: Jessica Diaz, Florida Department of Agriculture and Consumer Services, United States of America.

Figure 62. Mouthhook of *Anastrepha ludens*: with truncate posterior end (arrows).

Source: Jessica Diaz, Florida Department of Agriculture and Consumer Services, United States of America.

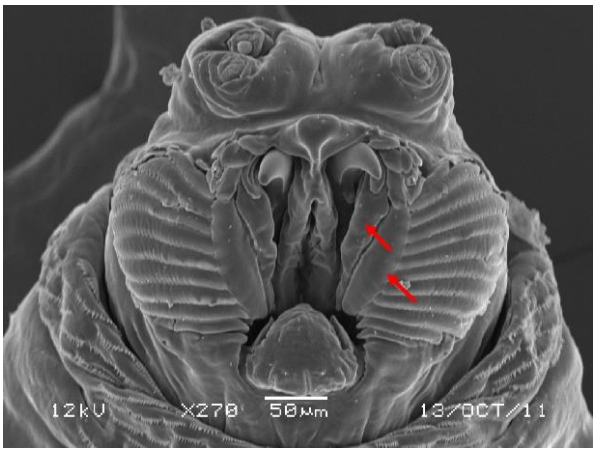

Figure 63. Facial mask of *Ceratitis anonae*: lateral lip divided into narrow inner and outer lips (arrows).

Source: Gary J. Steck, Florida Department of Agriculture and Consumer Services, United States of America.

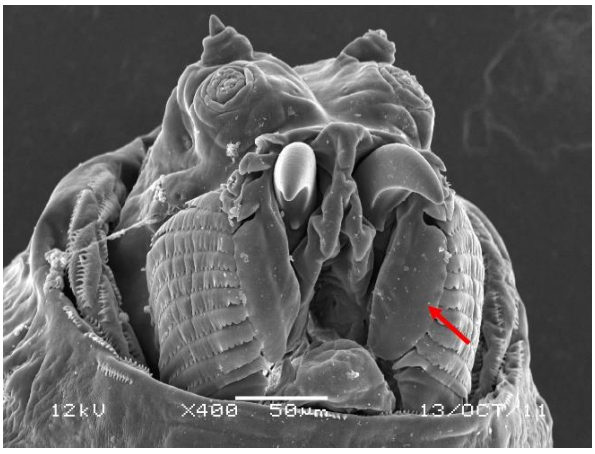

Figure 64. Facial mask of *Ceratitis capitata*: lateral lip wide and undivided (arrow).

Source: Gary J. Steck, Florida Department of Agriculture and Consumer Services, United States of America.

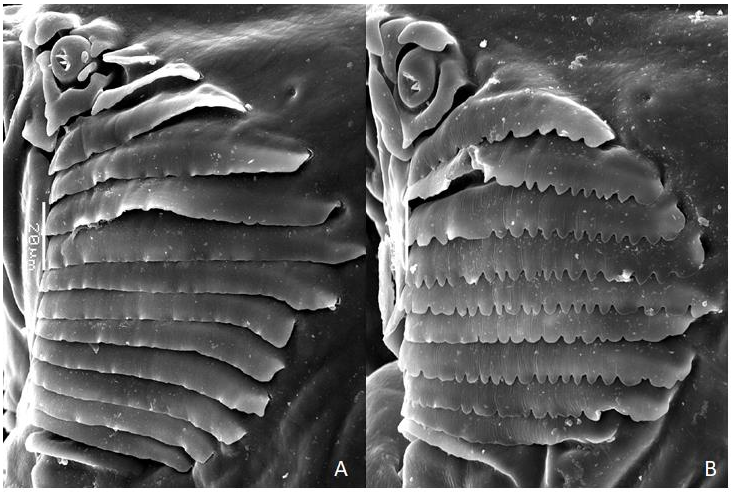

Figure 65. Oral ridges (left side) of *Ceratitis capitata*: (A) with entire margins and (B) with scalloped margins; no accessory plates.

Source: Louis A. Somma, Florida Department of Agriculture and Consumer Services, United States of America.

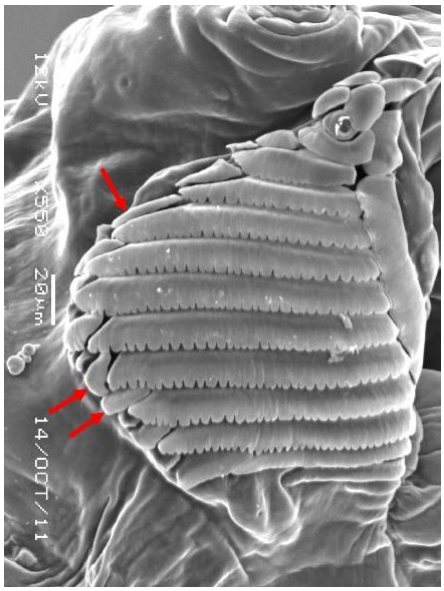

Figure 66. Oral ridges (right side) of *Ceratitis cosyra*: with scalloped margins; one series of accessory plates (arrows).

Source: Gary J. Steck, Florida Department of Agriculture and Consumer Services, United States of America.

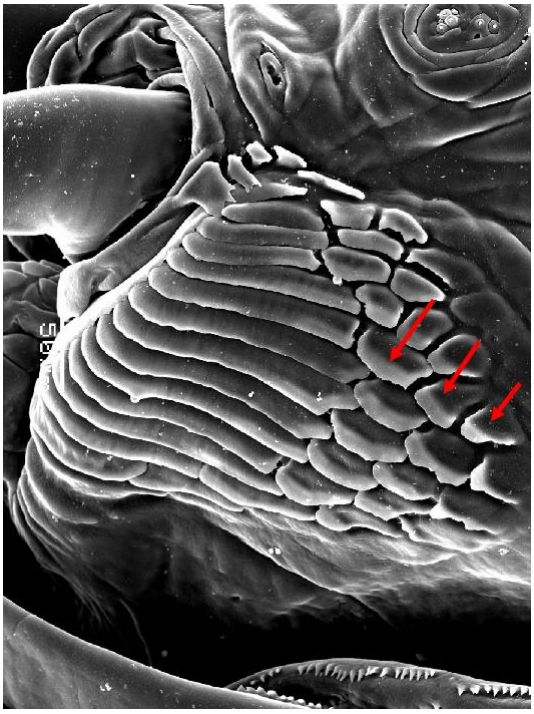

Figure 67. Oral ridges of *Anastrepha curvicauda*: with entire margins; three series of accessory plates (arrows).

Source: Louis A. Somma, Florida Department of Agriculture and Consumer Services, United States of America.

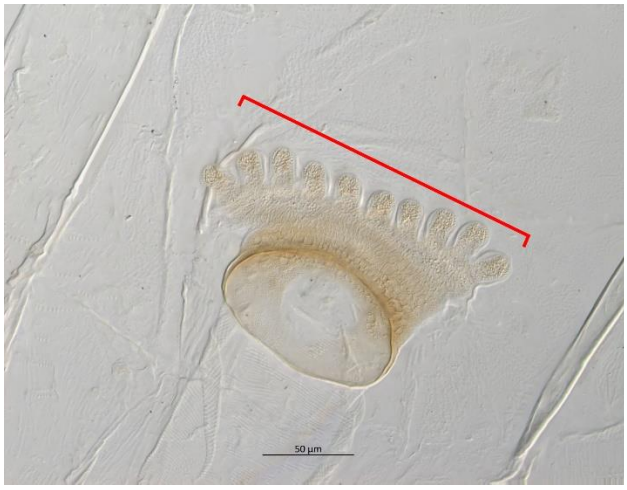

Figure 68. Anterior spiracle of *Ceratitis rosa*: flat topped. Red bar = apical width.

Note: Scale bar = 50 µm.

Source: Jessica Diaz, Florida Department of Agriculture and Consumer Services, United States of America.

Figure 69. Anterior spiracle of *Anastrepha ludens*: bilobed.

Source: Jessica Diaz, Florida Department of Agriculture and Consumer Services, United States of America.

Figure 70. Posterior spiracles of *Ceratitis anonae*. Arrows = length and width measurements.

Source: Jessica Diaz, Florida Department of Agriculture and Consumer Services, United States of America.

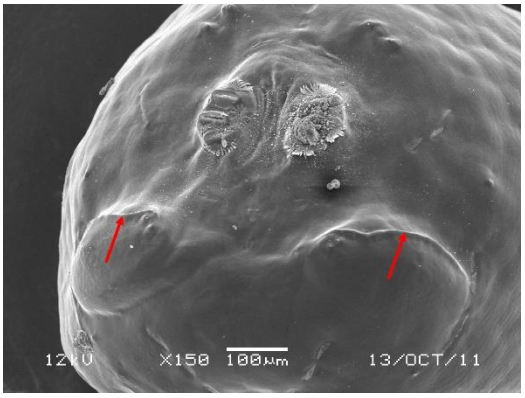

Figure 71. Caudal segment of *Ceratitis capitata*: caudal ridges present (arrows).

Source: Gary J. Steck, Florida Department of Agriculture and Consumer Services, United States of America.

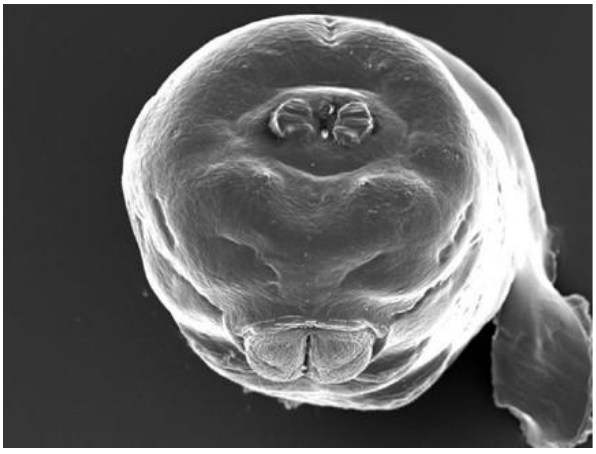

Figure 72. Caudal segment of *Anastrepha distincta*: caudal ridges absent.

Source: Louis A. Somma, Florida Department of Agriculture and Consumer Services, United States of America.

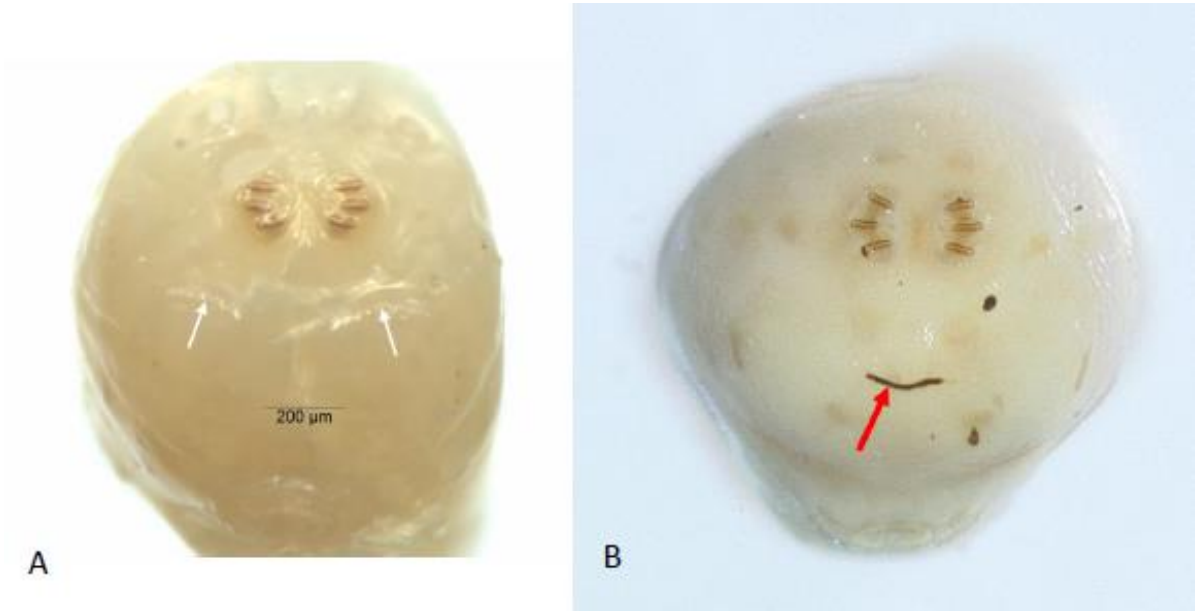

Figure 73. Caudal segments of (A) *Ceratitis capitata* with caudal ridges (arrows) and (B) *Zeugodacus cucurbitae* with black line (arrow) below caudal ridges.

Source: (A) Dale R. Traficante, Florida Department of Agriculture and Consumer Services, United States of America; (B) Gary J. Steck, Florida Department of Agriculture and Consumer Services, United States of America.

Publication history

This is not an official part of the standard

2016-05 Standards Committee (SC) added subject Genus *Ceratitis* (2016-001) to work programme.

2020-11 Technical Panel on Diagnostic Protocols (TPDP) agreed to recommend a change in scope of the draft DP to the SC.

2021-06 SC agreed to reduce scope of DP to diagnosis of the genus and six species.

2021-09 Expert consultation.

2022-04 TPDP recommended draft to SC to be approved for consultation.

2022-06 SC approved for consultation.

2022-07 Consultation.

2022-10 TPDP revised and recommended to SC for adoption.

2023-06 SC approved draft to be submitted to the 45-day DP notification period (2023_eSC_Nov_04).

2023-07 DP notification period (no objections received).

2023-08 SC adopted DP on behalf of CPM.

ISPM 27. **Annex 32**. 2023. Genus *Ceratitis*. Rome, IPPC Secretariat, FAO.

Publication history last updated: 2023-09

IPPC

The International Plant Protection Convention (IPPC) is an international plant health agreement that aims to protect global plant resources and facilitate safe trade.
The IPPC vision is that all countries have the capacity to implement harmonized measures to prevent pest introductions and spread, and minimize the impacts of pests on food security, trade, economic growth, and the environment.

Organization

- There are over 180 IPPC contracting parties.
- Each contracting party has a national plant protection organization (NPPO) and an Official IPPC contact point.
- 10 regional plant protection organizations (RPPOs) have been established to coordinate NPPOs in various regions of the world.
- The IPPC Secretariat liaises with relevant international organizations to help build regional and national capacities.
- The Secretariat is provided by the Food and Agriculture Organization of the United Nations (FAO).

International Plant Protection Convention Secretariat
ippc@fao.org | www.ippc.int

Food and Agriculture Organization of the United Nations
Rome, Italy